LAND AND WATER
www.csiro.au

The effect of grass curing and fuel structure on fire behaviour:

Final report

Miguel G. Cruz, Andrew Sullivan, Susan Kidnie, Richard Hurley, David Nichols

Report No. EP166414

September 2016

Prepared for the Country Fire Authority of Victoria

Citation

Cruz MG, Sullivan AS, Kidnie S, Hurley R, Nichols S, (2016) The effect of grass curing and fuel structure on fire behaviour - Final report. CSIRO Land and Water, Client Report No EP 166414, Canberra, Australia.

Copyright and disclaimer

Important disclaimer

Contents

Executive summary

Aims

We report on a field based study investigating the effect of grass fuel characteristics on fire behaviour potential, in particular:

- To quantify the effect of the degree of curing on grassfire spread, energy release and flame dimensions;
- To quantify the effect of the degree of curing on initial fire growth from a point source;
- To quantify the effect of fuel load on grassfire spread, energy release and flame dimensions;
- To evaluate current grass fire danger algorithms.

Experimental work

- The study used data collected in five experimental sites covering a large latitudinal gradient across Eastern Australia. The experimental sites were: Wangaratta South and Wendouree in Victoria; Tamworth and Braidwood in New South Wales (NSW); and Toowoomba in Queensland. The sites covered a spectrum of climates, prevalent fire weather, grass species and grass fuel structures.
- Three distinct experimental fire studies were considered: (i) fire spread sustainability burns (ii) linear fire propagation burns; and (iii) point ignition fire growth burns.
- A total of 12 fire spread sustainability experiments, 96 linear fire propagation experiments, and 26 point ignition experiments were conducted.

Results

- Sustained fire spread in grasslands was observed with curing levels between 20 and 30% when dead fuel moisture was below 10%.
- Fire spread rate in the fire behaviour experiments ranged from 2.8 to 100 m/min in the partially cured plots and the 6.2 and 150 m/min in the fully cured plots, with maximum fire intensity up to approximately 12000 kW/m.
- The data showed that none of the current operational curing coefficients performed well when compared to the curing effect observed in our experiments. The operational curing coefficients used in Australia, namely the one embedded into the Grass Fire Danger Rating System and the CSIRO Grassland Fire Spread meter, resulted in significant under prediction of the fire spread potential in partially cured grasslands of southern Australia.
- A new curing coefficient equation was proposed to predict fire spread and behaviour in southern Australia grasslands. This equation was evaluated against newly collected independent data, showing adequate prediction capability and absence of bias.
- We investigated the effect of fuel load on grassland fire behaviour. Fuel load was not found to influence fire rate of spread or flame height.

- We found the curing function implemented in the McArthur Mk 4 Grassland Fire Danger Meter to result in under estimation of fire potential by a factor of three.
- We evaluated the use of the Purton (1982) modified Mk 4 Grassland Fire Danger Meter fuel load function in the calculation of GFDI and found this formulation to not be supported by data and to artificially bias the results, potentially leading to misleading fire danger warnings.

Management implications

- Our results suggest that the fire spread curing function developed and evaluated in the current project is clearly more accurate than previous functions. In light of the evidence collected in this study we recommend the new function be implemented for operational prediction of grassland fire behaviour.
- In light of the long held beliefs regarding the effect of curing level on fire behaviour, it is recommended that new training materials be produced to highlight the new knowledge produced in the current work, namely that sustained propagation can occur in levels of curing as low as 25-30%, and that fires in partially cured pastures will spread faster than previously believed in partially cured grasslands.
- Our results show that under the right weather conditions, fire in grasslands with reduced fuel load (between 0.15 and 0.25 kg/m^2) can exhibit high intensity fire behaviour, with very fast rates of spread and deep flame fronts. It is also advised that the results from the investigation of the effect of fuel load on fire behaviour be communicated to fire-fighters.
- The results show that the strong curing damping effect implemented in the current fire danger model produces an under-evaluation of fire potential when fires occur under dry and windy conditions in partially cured grasslands. The results show an under prediction by a factor of 3. A re-evaluation of the current system for fire danger in grasslands is advised.
- The results of the study should be communicated to fire agencies across Australia so they can be utilised in future policy, fire fighter training and information to assist in educating the rural community through warnings and messaging.

Acknowledgments

The authors are grateful to Country Fire Authority (CFA) of Victoria, and in particular Alen Slijepcevic, for supporting this research project on grass curing and structure on fire behaviour. The authors thank also the NSW Rural Fire Service, in particular Laurence McCoy, and Queensland Fire and Emergency services, in particular Andrew Sturgess, for their contributions to this project.

For the Victorian burns, the authors are grateful to Jude Alexander, Tony Brady, Veronica Clifford, Graham Coulson, Martyn Ellis, Kelsy Gibos, Vijay Koul, Maree Larkin, Danielle Martin, Dominic Uljanic, Ingrid Welles and Martin Wyschka for their contribution to this project. Appreciation is also extended to Graham Coulson and the City of Ballarat for providing the experimental sites, and local CFA brigades for the in-kind support.

For the New South Wales burns, appreciation is extended to the Tamworth site owner, Single Builders (namely Mark Single) and Braidwood site owner, Water NSW (namely Tony Kondek) and its lessee Jamie Ramm. We also thank the various RFS collaborators, namely, Barry Gehrig, Allyn Purkiss, Phil Paterson, Tim Carrol, Chris Quinn, Steve Prior, Jessica Wells, David Field, Belinda Kenny, David Philp, Andrew Jones, Levi Roberts, Wendy Smith and Simon Louis. We also thank the support of the local Rural Fire Service brigades.

For the Queensland burns, appreciation is extended to Barry Brazel and the Department of Transport and Main Roads, Barry Brazel, Eddie Lacko, Russell Stephens-Peacock, Simon Dawson, Casey Scholten from Queensland Fire and Emergency services, and the local fire brigades that provided the required fire suppression activities.

We also thank the collaboration of Jim Gould (CSIRO), Matt Plucinski (CSIRO), Rachel Bessell (CFA, Victoria) and Tim Wells (CFA, Victoria).

The project recognises the support provided by the Commonwealth Attorney-General’s Department through a National Emergency Management Program project grant.

1 Introduction

One of the keys to understanding fire susceptibility in grasslands is to know their annual growing cycle, and in particular, how senescence affects the biomass available for combustion. Grass senescence is a sequential process where the remobilization of nutrients from older plant components to new leaves or to support reproductive development lead to the death of plant organs or the whole plant. As senescing progresses, the fuel moisture content gradually decreases and the proportion and amount of dead material increases, raising the general “combustibility” of a grassland fuel type (Cheney and Sullivan 2008). The proportion of dead fuel material in a grassland is typically described as curing level (as a percentage) (Luke and McArthur 1978; Anderson *et al*. 2011) or the live to dead fuel load ratio (e.g. Fosberg and Schroder 1971; Rothermel 1972). Grass curing has been found to have a significant effect on fire behaviour in grasslands (e.g. McArthur 1966, Cheney *et al*. 1998). In Australia, where grasslands cover approximately 75% of the country (Cheney and Sullivan 2008), the degree of curing has been used as an input into the calculation of grassland fire danger ratings (McArthur 1966) and grassfire spread (Cheney *et al*. 1998). The ability to accurately assess the degree of curing is therefore important for fire agencies that are responsible for predicting fire danger throughout the year.

An early study by the authors reported on the results from an experimental field burning campaign in southern Australia temperate grasslands, namely in Wangaratta and Ballarat, Victoria (Kidnie et al. 2015; Cruz et al. 2015). These authors found both the current methods used to estimate curing level and the effect of curing level on fire behaviour to misrepresent observed results. In 2015, we aimed to extend the study approach to grasslands with different growth dynamics and fuel structures. Sites were selected in NSW and Queensland. In the autumn of 2014 two experimental burns took place in Tamworth, NSW and Toowoomba, Queensland. In the summer of 2015, a final set of experimental burns were completed in Braidwood, NSW.

2 Methods

2.1. Study sites

Five experimental sites were located across eastern Australia: Wangaratta South (36°24′7.4″S, 146°14′57.9″E) and Ballarat (37°31′12.9″S, 143°48′3.4″E) in Victoria; Tamworth (31˚ 2′ 15.09″S, 150˚ 54′ 47.38″ E) and Braidwood (35° 18' 56" S, 149° 43' 22" E) in New South Wales; and Toowoomba (27˚ 30′ 38.96″S , 151˚ 52′ 47.63″ E) in Queensland. A continuous grass cover, a requirement for the purposes of studying grass curing dynamics and fire behaviour, characterized all sites selected.

The fire weather climatology for each site was studied to define the plot layout, so that plots were aligned with the direction of the most consistent winds under the range of expected burning conditions for conducting the experiment fires.

The Wangaratta South site was situated north of the Great Dividing Range in the Northern Inland Slope bioregion (Parkes *et al.* 2003). The site was located 173 m above mean seal level (AMSL) in an open, fully exposed improved pasture dominated by annual rye grass (*Lolium rigidum* Gaudin) and Yorkshire fog grass (*Holocus lanarus* L.). The majority of grasses were visually assessed as coarse with respect to diameter width. Fuels were not clumpy in nature. The soil type was classified as a chromosol (Northcote *et al*. 1968). Average annual rainfall in the area is 609 mm and average monthly mean temperatures ranges from 13°C (in July) to 32°C (in January). The Wangaratta South site had 42 plots (Figure 1) and experimental burns were carried out between November and December 2013.

The Ballarat site was located in the Victorian Volcanic Plain bioregion (Parkes *et al.* 2003) at a height of 454 m AMSL. The site was open, generally flat, with an improved pasture dominated by sweet vernal grass (*Anthoxanthum odoratum* L.), annual ryegrass (*L. rigidum* G) and brown-top bent grass (*Agrostis capillaris* L.). Grasses were visually assessed as predominantly fine in respect to diameter width. Fuels were not clumpy in nature. At this site the soil type is classified as a sodosol (Northcote *et al*. 1968). Average annual rainfall is 694 mm and average monthly mean temperatures range from 10°C (in July) to 25°C (in January). The site had been harvested the previous season and a couple of centimetres of dead grass remained throughout the site. The Ballarat site had 55 plots (Figure 2) and experimental burns were carried out between December 2013 and January 2014.

The Tamworth site was located west of the Great Dividing Range in the Nandewar bioregion (Parkes *et al.* 2003) at a height of 446 m AMSL. The site was an open, improved pasture. Grasses were visually assessed as predominantly coarse in respect to diameter width. Fuels were mostly clumpy in nature, but continuous. Average annual rainfall in the area is 636 mm and mean temperatures range from 16°C (in July) to 33°C (in January). The site had not been harvested in the previous season and previous seasons's growth remained. The Tamworth site had 30 plots (Figure 3) and experimental burns were carried out in March 2015.

Figure 1. Wangaratta experimental area showing arrangement of 33 x 33 m plots. Darker areas have already been burnt. Paler plots are fully cured plots attained through the use of herbicide treatment.

Figure 2. Ballarat experimental area showing arrangement of 33 x 33 m plots. Darker areas have already been burnt. Paler plots are fully cured plots attained through the use of herbicide treatment.

Figure 3. Tamworth experimental area showing arrangement of 33 x 33 m plots. Darker areas have already been burnt. Paler plots are fully cured plots attained through the use of herbicide treatment.

The Braidwood site was located west of the Great Dividing Range in the South Eastern Highlands bioregion (Parkes *et al.* 2003) at a height of 626 m AMSL. The site was an open, fully exposed improved pasture with a number of pasture species mixed throughout the site. Grasses were visually assessed as a mixture of coarse and fine in respect to diameter width across the site. Fuels were not clumpy in nature. Average annual rainfall in the area is 640 mm and mean temperatures range from 12°C (in July) to 27°C (in January). The site had been harvested the season previous to the burns and had very little previous seasons growth remaining. A total of 74 plots (Figure 4) were prepared at this site. Burns were carried out in December 2015.

The Toowoomba site was located west of the Great Dividing Range in the Brigalow Belt South bioregion (Parkes *et al.* 2003) at a height of 524 m AMSL. The site was generally flat with improved pasture. Grasses were visually assessed as predominantly fine in respect to diameter width. Fuels were predominantly clumpy in nature. The soil type is classified as a volcanic. The area has a subtropical highland climate with warm summers and mild winters. Average annual rainfall is 726 mm and average monthly mean temperatures range from 17°C (in July) to 28°C (in January). The site had been left undisturbed for the year prior to burning resulting in previous season's growth remaining onsite. The Toowoomba site had 20 plots (Figure 5) and experimental burns were carried out in April 2015.

Figure 4. Braidwood experimental area showing arrangement of 33 x 33 m plots, some of which have been already burnt.

Figure 5. Toowoomba experimental area showing arrangement of 33 x 33 m plots. Paler plots in the left (4) and in the bottom right side of image are fully cured plots attained through the use of herbicide treatment.

2.2. Experimental design

Three different sets of field experiments were conducted to quantify the effect of curing level on distinct aspects of fire behaviour:

- **Fire spread sustainability** experimental burns aimed to quantify the effect of curing on the likelihood of sustained fire propagation at low levels of curing (i.e., 20-50%).
- **Linear fire propagation** experiments consisted of individual or simultaneously ignited burns lit from continuous lines to investigate the effect of curing in key fire behaviour properties, such as rate of fire spread, flame height, flame depth, fireline intensity and residence time. Data from these experiments was also used to investigate the effect of other fuel structure variables, such as fuel load and height, on fire behaviour.
- **Point ignition fire growth experiments** consisted of individual or simultaneously ignited burns lit from single points aimed at quantifying the initial growth rate of point source fires and its dependence on curing level.

Fire sustainability burns

The fire sustainability experiments comprised so-called ‘go/no-go’ experiments burnt under low curing levels. These experiments were aimed at exploring the likelihood of sustained fire propagation in the early stages of plant senescence (i.e. a degree of curing of 20 to 50%). Fire sustainability experiments preceded the main set of fire propagation experiments.

The experimental design called for these burns to commence when visual curing levels of 30% were attained. Plots 20 x 20 m (0.04 ha) in size were ignited under a range of environmental conditions and degree of curing levels. The ignition line was set on the upwind side of the plot in order to capture the wind-driven fire propagation. Approximately 15 minutes prior to the scheduled ignition time, the position of the 20 m long ignition line was determined according to prevailing wind direction. If fires failed to spread at this curing level, a new set of fire sustainability experiments were conducted when the degree of curing increased by about 10% (i.e. to a 40% visual curing level). The process was repeated until sustained fire spread was achieved (i.e. when a continuous flame front spread across the 20 m plot distance). After this occurred, the experimental work would focus on the linear fire propagation experiments which focused on fire behaviour measurements.

Linear fire propagation burns

The experimental design for the linear fire propagation aspect of the study called for simultaneous fires conducted in 100% cured (control; obtained by desiccating the pasture with herbicide) and partially cured (treatment; grasses curing naturally as determined by environmental controls) plots over a range of curing levels.

The control plots were treated with a systemic herbicide (glyphosate). The herbicide treatment was applied when height growth and seed head development were completed. The timing of the herbicide treatment aimed also to have the control plots fully cured (i.e. all plants dead) when the remaining plots were approximately 30% cured based on a visual assessment. The herbicide application was preceded by laboratory tests in a cone calorimeter (Brabauskas 1984, 2003) to investigate if the application of herbicide would change the flammability of the grasses. In these tests no significant differences in time to ignition and mass loss rate were observed between the herbicide treated and untreated grass fuels.

The size of the experimental plots was constrained by the maximum length of the available agricultural crop sprayer boom (Fig 6-top) used to apply herbicide. From the first series of experiments (Wangaratta and Ballarat) a plot size of 33 x 33 m (0.1 ha) was selected. Plots were separated by a 3 m short mown grass fuel break. At the Braidwood site, failure to contract a suitable wheeled agricultural crop sprayer, led to the use of an aerial sprayer (Fig. 6-bottom). The aerial sprayer platform was faster and cheaper than the previously used tractor based crop sprayer.

Ignition of these experiments was planned to be based on a line fire ignited in the upwind edge of a plot. In situations where wind direction was not aligned with the plot, corner ignitions were conducted.

Figure 6. Top - Crop sprayer used at the Ballarat site. Bottom – helicopter sprayer used at the Braidwood site.

Point ignition fire growth experiments

These experiments were aimed at quantifying the effect of curing level on the growth rate, or build up, of a fire ignited by a point source. Plot layout and experimental design was as described above for linear fire experiments with the exceptions that (1) ignition was a point source ignition instead of a continuous line; and (2) a handful of experiments were conducted in plots measuring 69 x 33 m. Ignition from a single point better represents the outbreak of a fire, either natural, accidental or deliberate in nature. Location of the ignition was decided just prior to ignition to maximise fire spread across the experimental plot.

2.3. Fuel assessment

2.3.1. Fuel structure and curing level

Grass fuels were sampled for physical structure (load by state, height, compactness) and curing level. Four fuel sampling areas were systematically located within each experimental fire plot. In each of these areas, visual assessment of curing following the Victorian Country Fire Authority Grassland Curing Guide (CFA Fire and Emergency Management 2014) and a measurement of grass height were recorded prior to the destructive sampling. Fuels within a 0.25 m^2 quadrat (0.5 x 0.5 m) were clipped down to ground level. Depending on the amount of fuel present in the quadrant, between one-quarter and one-half of the quadrat was separated for sorting.

Grass fuel components were partitioned into four distinct fuel categories: (i) old dead, (ii) new dead, (iii) senescing and (iv) green. Old dead (*od*) is the grass fuel component from the previous year's growth. The structure and appearance of this fuel component depends on previous land use, age and grass species. Undisturbed (i.e. ungrazed and unharvested) old dead grass generally forms a matted horizontally-oriented layer close to the ground. In tussock grasses old dead fuel and new growth are intermixed, and new grass growth develops through the old dead fuel. In this tussock grass case, much of the old dead fuel is vertically-oriented. In grasslands that have been harvested or heavily grazed, only a few centimetres of vertical stalk remains. Fuel particles of this component have a colour varying from light to dark brown or grey, depending on species and age. New dead (*nd*) is the dead fuel component from the current season's growth. These fuels are usually attached to living fuel and maintain their vertical structure before full curing is reached. There is no remaining green chlorophyll pigment present. Thus, they appear bleached and the stalks break easily. Moisture content in the *od* and *nd* fuel components closely follows environmental conditions. Senescing (*sen*) fuels are undergoing transition from live to dead. Fuel colouration in the senescing category depends on the amount of chlorophyll pigment remaining and can range from pale green to green-yellow or yellow in colour. Components in this category do not break as easily as *nd* fuels but they also do not feel as lush as green fuels. Green (*g*) fuel is the component that is green in colour and does not show any obvious physical signs of plant tissue deterioration or aging. Leaves in the green category are generally soft to the touch and stalks show visible moisture if broken.

In partially-cured grasses, it was often necessary to separate a single piece of grass into multiple fuel components. For example, the bottom third of the grass stalk may still be fully green, the top two thirds of the stalk may appear dead, but upon closer examination, the stalk is senescing, with a dead sheath covering the senescing fuel and extending out to dead leaf tillers.

After sorting, all fuel components from the subsample were separately oven-dried for 24 h at nominal temperature of 105°C for dry weight estimation (Matthews 2010); after which the proportions (between zero and 1.0) of each of the four fuel components was determined. The unsorted fuel was oven-dried using the same method to determine total fuel load. The total of the two separate samples were combined and the load of each fuel component was computed by applying the sub-sample calculated component proportion to the total fuel load.

The degree of curing (*C*, %) was calculated as follows:

$$C = 1\frac{w_{od} + w_{nd}}{w_{od}+w_{nd}+w_{sen}+w_g}\times 100 \qquad [1]$$

where *w* is the weight of fuel (kg/m^2) and the suffix denotes the fuel component defined above.

2.3.2. Fuel Moisture Content

Fuel moisture content samples were collected separately from the fuel structure samples. Three samples (20 – 30 g each) were collected per fuel component and sealed in airtight metal tins. Samples were later weighed (w_{wet}), oven-dried for 24 hours at 105 °C and then reweighed (w_{dry})(Matthews 2010). Fuel moisture was expressed as a percentage of oven dried weight (M_i):

$$M_i = \frac{w_{wet}-w_{dry}}{w_{dry}} \times 1002 \qquad [2]$$

Overall fuel moisture (i.e. all four categories combined (.M_{all}) was calculated as a weighted average taking into account the proportion (Π_i) of each fuel component category and its moisture content (M_i):

$$M_{all} = 3\sum_{i=1}^{n=4}\Pi_i M_i \qquad [3]$$

The pooled moisture content of live fuels was calculated similarly, but only talking into account the green and senescing fuel component categories. Dead fuel moisture content refers to the new dead fuel component category.

2.4. Weather measurements

An automatic weather station measuring air temperature, relative humidity and solar radiation at 1.5 m above ground at 10-min intervals was established at each experimental site. Wind speed and direction at 2 and 10-m height were measured with 2-D sonic anemometers. Data was sampled and logged at a frequency of 10Hz.

For each individual burn, two, or sometimes one, 2-D sonic anemometers were located approximately 35 m up-wind of the ignition line. Wind speed and direction were sampled and logged at 10Hz.

2.5. Experiment ignition

The experimental fires were timed to coincide with the period of daily strongest forecasted wind speeds consistent with the plot alignment and the time of minimum dead fuel moisture. Operational constrains led to ignitions earlier or later in the day at times. Fires were ignited on the upwind edge of each plot. Prior to ignition, fire suppressant (water of Class A foam) was applied to the fuel breaks that surrounded the unburnt plots.

For fire sustainability and linear fire propagation experiments, a line source ignition was achieved by a team of two igniters carrying hand-held drip-torches, and travelling from a corner towards the centre of a plot. It generally took 10-15 sec to set a continuous flame front that would ensure a well-developed flame front and steady state propagation by the time the fire reached half of its intended run.

For point ignition burns, a sole ignition point was achieved by using a match. The location of the ignition point depended on the strength, direction and consistency of the prevailing winds, aiming to ensure the longest possible run within the experimental plot.

2.6. Fire behaviour measurements

The behaviour of each experimental fire was monitored using in-situ instrumentation, ground based and aerial videography and visual observations by experienced fire behaviour observers. Measurements varied between type of experiment, with the linear propagation experiments being the most highly instrumented. Fire behaviour observers in close proximity to the flame front monitored various flame front characteristics throughout each experimental burn. The fire behaviour characteristics recorded by the observers were: flame geometry (depth, height and angle), fuel responsible for propagation and the duration of in-draught winds (i.e. lulls in fire propagation).

2.6.1. Rate of fire spread

Rate of fire spread was determined from measurements of the time of fire arrival at plot grid points (grid spacing 7.5 x 7.5 m or 10 x 10 m) within each experimental plot. Time of fire arrival was assumed to coincide with a temperature of 320°C (Albini 1985) measured by 1.5-mm diameter, type K metal-sheathed thermocouples (Pyrosales, NSW, Australia) connected to small dataloggers (HOBO® U12, Onset, MA, USA) buried in the ground. Thermocouple size and characteristics was a compromise between response time and durability. Loggers sample temperatures at 1 Hz.

Aerial imagery captured with use of unmanned aerial vehicles (UAV; DJI Phantom Vision and Phantom 3) was also used to derive fire isochrones from which rate of spread could be estimated.

2.6.2. Fireline intensity

Fireline intensity (I_B, kW/m), the rate of energy release per unit time per unit length of fire front, was calculated as per Byram (1959):

$$I_B = hw_aR \qquad [4]$$

where R is the fire rate of spread (m/s), w_a the fuel consumed in flaming combustion (kg/m^2), assumed to be all fuels, and h the heat released by the combustion of fuel (assumed 18,700 kJ/kg). Corrections for fuel moisture were applied, 1263 kJ/kg for the latent heat absorbed when the water of reaction is vaporized, and 24 kJ/kg per moisture content percentage point (Byram 1959; Alexander 1982)

2.6.3. Flame dimensions

Flame height and flame depth were estimated from direct measurements. Two 1.5 m vertical markers were place 10 meters apart close to the end of the experimental plot to be used as visual references from which flame height could be estimated. For a given fire, flame height was estimated from a series of digital photographs (shutter speed = 400/sec) taken from a fixed point that had both vertical makers within the field of view (Figure 7) (Adkins and Clements 1976; Britton et al. 1977; Clements et al. 1983).

Flame depth (F_D) was inferred from the product of rate of spread by residence time as per:

$$F_D = R \cdot \tau_r \quad [5]$$

Flame length and angle measurement were not quantified due to the difficult in determining the flame depth mid-point in high intensity fires (see figure in Box 1).

Figure 7. Example of flame size and angle variability as it spreads between flame markers (1.5 m tall).

2.6.4. Residence time

Residence time, the length of time required for the flaming zone of a spreading fire to pass a given point, was estimated from the time-temperature profile measured at a selected number of fires with small diameter bare wire type K thermocouples (0.125 mm wire diameter/0.25 mm bead diameter – Omega Corporation, USA). Data was acquired at 10 Hz. Residence time was defined as the time temperature remained above 320C, a nominal threshold temperature for piloted ignition of wildland fuels (Albini 1985).

Box 1: Idealised flame dimensions

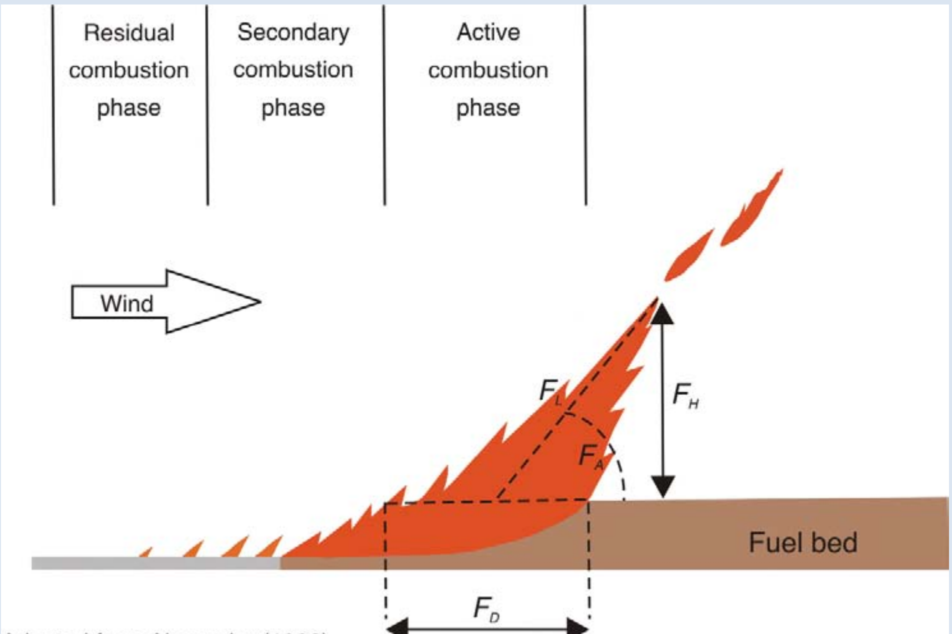

Flame height (F_H): The average maximum vertical extension of flames at the fire front; occasional flashes that rise above the general level of flames are not considered.

Flame depth (F_D): The width of the zone within which continuous flaming occurs behind the edge of the fire front.

Flame length (F_L): The length of flames measured along their axis at the fire front; the distance between the flame height tip and the midpoint of the flame depth. Within a given fuel type, flame length is proportional to fireline intensity.

Flame angle (F_A): The angle formed between the flame at the fire front and the ground surface.

Flame residence time (τ_r): The length of time required for the flaming zone of a spreading fire to pass a given point.

Heat per unit area (H_A): the heat release per unit area; the product of total fuel consumed (w) and the heat release by the combustion of fuel (h).

Definitions from Merril and Alexander (1987)

2.6.5. Fire shape and growth

Fire shape and rate of growth were derived for the point ignition experiments from UAV footage (Figure 8. Top- Raw oblique aerial imagery of fire S13 at Braidwood approximately 90 seconds after ignition. Bottom- Spatially rectified and trimmed image used for fire perimeter digitisation and rate of spread measurements.

A). This footage was corrected for image distortion (i.e. spatially rectified to present as planar an image as was possible within the limits of the original footage) and trimmed (Figure 8. Top- Raw oblique aerial imagery of fire S13 at Braidwood approximately 90 seconds after ignition. Bottom- Spatially rectified and trimmed image used for fire perimeter digitisation and rate of spread measurements.

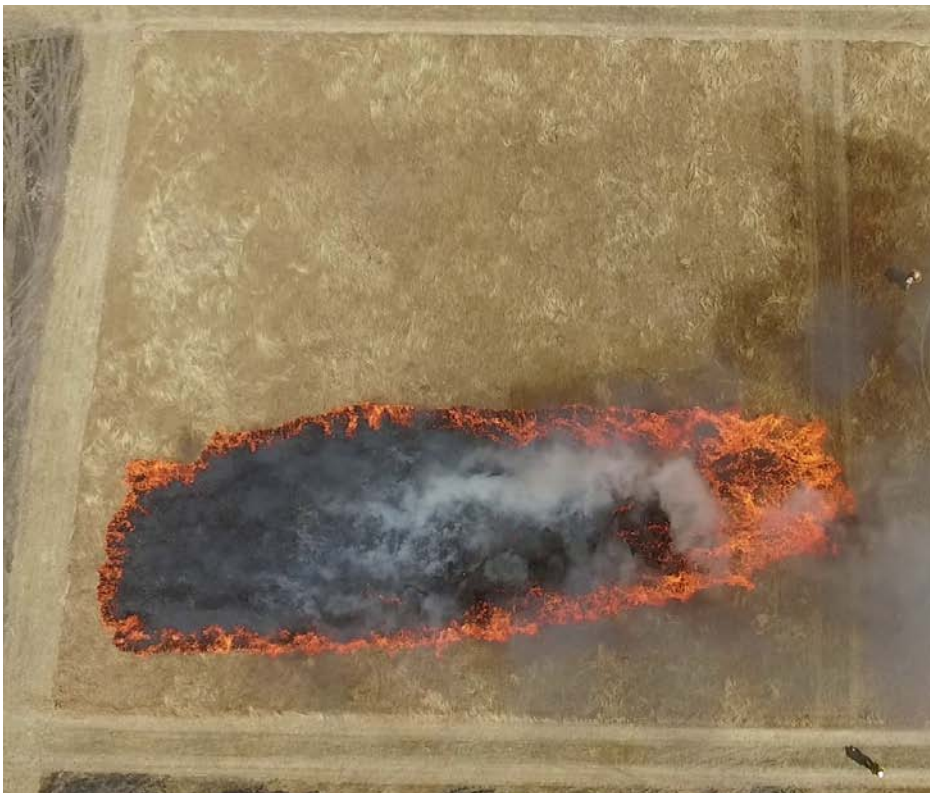

Figure 8. Top- Raw oblique aerial imagery of fire S13 at Braidwood approximately 90 seconds after ignition. Bottom- Spatially rectified and trimmed image used for fire perimeter digitisation and rate of spread measurements.

B) using purpose built software in the CSIRO Workspace environment (http://research.csiro.au/workspace/) that utilises the OpenCV2 video analysis editing library (Bradski 2000).

Still images were extracted from the UAV video at regular intervals (generally every 10 s) using a Python script also based on CV2. Fire perimeter and burnt out area within the fire perimeter were then manually digitised using WebPlotDigitiser v3.8 (http://arohatgi.info/WebPlotDigitizer), enabling an expert assessment of fire edge location that may be occluded by tall flame or smoke. The resolution of manual digitisation depended upon fire size and complexity but the average spacing between points used to define the fire perimeter was between 3 and 8 cm (Figure 9).

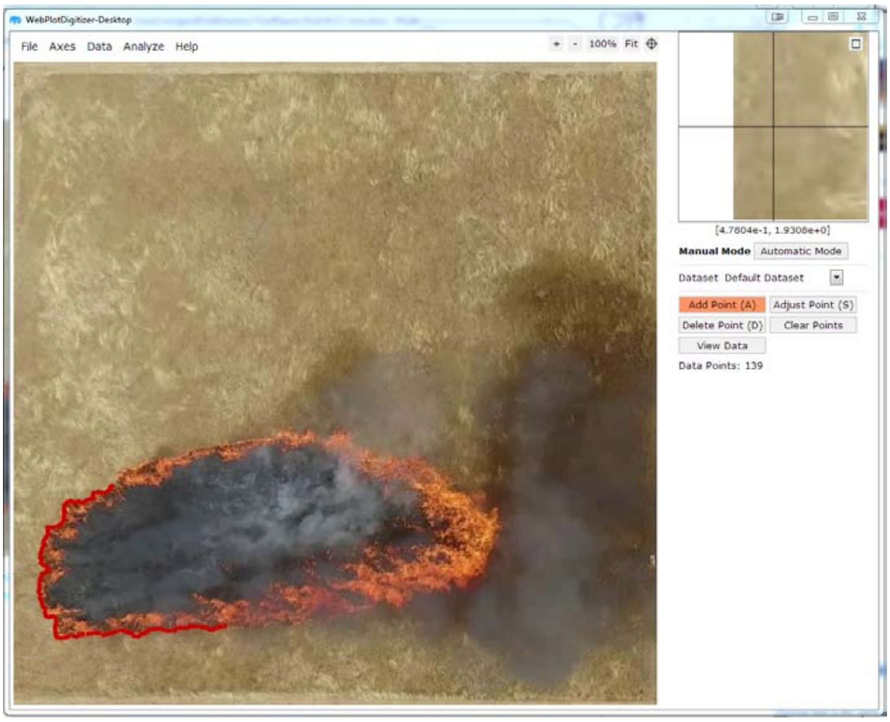

Figure 9. Example of the digitisation process used to convert a rectified still image of a fire at a particular time to data. Each red point represents one point in the polygon that will represent the fire perimeter at this time.

Fire behaviour metrics such as area, perimeter length, as well as rate of change in these quantities were calculated directly from these data using an R script as was a fire isochrone map in which fire perimeters at each time interval were plotted. From each isochrone in the isochrones map additional fire behaviour metrics such as cumulative and interval distance and angle travelled, fire shape (length and breadth) and orientation, and headfire width (see Cheney et al. 1993) were measured for each time step using the image analysis and processing software ImageJ (http://imagej.nih.gov/il). From these metrics, length to breadth ratio, cumulative and interval rate of spread, were calculated.

2.7. Fire modelling

2.7.1. Curing Factor

For each burn pair we calculated the ratio between rate of fire spread measured in the partially cured and fully cured plots, respectively R_C (treatment) and $R_{100\%}$ (control):

$$\Theta_C = \frac{R_C}{R_{100\%}} \quad [6]$$

This curing coefficient, Θ_C, represents the reduction in rate of spread in partially cured grasses from a benchmark fully cured condition. This ratio is equivalent to the curing coefficients used in Cheney *et al*. (1998) and Wotton *et al*. (2009) functions.

Similarly, the effect of curing on fireline intensity and flame height was quantified through a ratio between the fire quantity measured in the treatment and the control:

$$\Theta_C = \frac{I_C}{I_{100\%}} \quad [7]$$

$$\Theta_C = \frac{FH_C}{FH_{100\%}} \quad [8]$$

2.7.2. Evaluation of existent curing coefficient functions

In previous work based on the Wangaratta and Ballarat datasets, Cruz et al. (2015) developed a new curing coefficient function for rate of fire spread:

$$\Phi C = \frac{1.036}{[1+103.99\exp(-0.0996\,(C-20))\,]} \quad [9]$$

In the current report we aimed to evaluate this function with the Tamworth, Toowoomba and Braidwood datasets. Concurrently, we will use these datasets to further evaluate previous curing functions:

McArthur (1966, 1973) Grassland Fire Danger Meter Mk ¾:

$$\Phi_{GFDI} = 2\,(C^{5.01})\,exp(-23.765) \quad [10]$$

Cheney et al. (1998):

$$\Phi C = \frac{1.12}{[1+59.2\exp(-0.124\,(C-50))\,]} \quad [11]$$

Wotton et al. (2009):

$$\Phi C = \begin{cases} 0.005\,(exp(0.061\,C)-1), & \text{if } C \leq 58.8 \\ 0.176 + 0.02\,(C-58.8), & \text{if } C > 58.8 \end{cases} \quad [12]$$

Model fit was assessed using the following goodness-of-fit statistics: root mean squared error (RMSE), mean absolute error (MAE), mean bias error (MBE) and the mean absolute percentage error (MAPE) (Willmott 1982; Mayer and Butler 1993).

2.7.3. Evaluation of flame height models

We evaluated the grassland flame height model developed by Cheney and Sullivan (2008) based on experimental data collected at Annaburroo Station, NT (Cheney et al. 1993; 1998). Following the fuel condition assumptions used in the rate of fire spread formulation, the proposed flame height models are applicable for (1) ungrazed grasses and (2) grazed or cut grasses. Here we evaluated the ungrazed grasslands formulation:

$$FH = 2.66\left(\frac{R}{60}\right)^{0.295} \quad [13]$$

where R is the rate of spread in m/min and FH is flame height in meters. Goodness of fit statistics used were those described in section 2.7.2.

2.7.4. On the effect of fuel structure on rate of fire spread and intensity

The effect of fuel load and other fuel structure variables on rate of fire spread were analysed through non-linear regression analysis. Given the dominant effect of wind speed and dead fuel moisture content on fire spread, we used well-accepted functional forms to describe the effect of these variables, namely a power function of wind speed and an exponential decay function of dead fuel moisture content as in Cheney et al. (1998), Cruz et al. (2013), and Anderson et al. (2015). We then add fuel structure variables, such as fuel load or height, to the model and test for their significance. The model form is:

$$R = a\, U_2{}^{b}\, exp(-c\, M_d)\Theta_1(V_1) \ldots \Theta_p(V_p) \qquad [14]$$

where *R* is the rate of spread, *a* and *b* are constants, U_2 is the wind speed at 2 m, M_d is the dead fine fuel moisture content. $\Theta_1(V_1) \ldots \Theta_p(V_p)$ are the product of functions of *p* fuel structure variables, V1..V_p and *p* is the number of statistically significant variables in the model. The functions, Θ_i, were either power or exponential functions, depending on the most sensible formulation. Regression analysis used the software R (R Core Team 2014).

2.7.5. On the effect of fuel structure on Grass Fire Danger Index

A number of distinct interpretations of the concept of fire danger rating exist worldwide. In Australia, the Grassland Fire Danger Index (GFDI) was originally related to fire spread rate and the fire danger rating was derived from Alan G. McArthur's expert assessment of suppression difficulty in average pastures (Table 1) (McArthur 1966; Cheney and Gould 1995). GFDI was calculated from Noble et al. (1980) parameterization of the Mk 3 circular meter:

$$GFDI = 2\, exp(-23.6 + 5.01\, ln(C) + 0.0281\, T - 0.226\, \sqrt{RH} \;+\; 0.633\, \sqrt{U_{10}}) \qquad [15]$$

where C is the curing level, T is air temperature, RH is relative humidity and U_{10} is the average wind speed measured at 10-m in the open.

Purton (1982) calculated GFDI from the Mk 4 Grassland Fire Danger meter as:

$$GFDI = exp(-1.523 + 1.027 log(W_a) - 0.009432\, (100 - C)^{1.536} + 0.02764\, T - 0.2205\, \sqrt{RH} + 0.6422\, \sqrt{U_{10}}) \qquad [16]$$

where the fuel load (W_a) function is that derived from the Mk 5 linear meter. As can be seen, particular in regard to the *T*, *RH* and U_{10} variables, these two functions are very similar, suggesting that the differences are only slight and perhaps due to slight variations in the construction of the cardboard meters from which the data were extracted.

Table 1. McArthur (1966) fire danger classes and interpretation after Cheney and Gould (1995).

Fire danger Class	Fire danger index	Rate of spread at max FDI in class (km/h) [m/min]	Difficulty of suppression
Low	0 – 2.5	0.3 [5]	Headfire stopped by roads and tracks
Moderate	3 – 7.5	1.0 [17]	Headfire easily attacked with water

High	8 – 20	2.6 [43]	Head attach generally successful with water
Very High	20.5 – 50	6.4 [110]	Heat attach may fail except under favourable circumstances.
Extreme	50 – 100/150	12.8 [215]	Direct attach will generally fail – backburns difficult to hold because of blown embers.
Above Extreme/catastrophic/code red	>150	Not defined	

3 Results

3.1. Exploratory data analysis

A total of 143 experimental fires were conducted. Of these, 12 were fire sustainability experiments, 105 were fire spread experiments and 26 point source fire growth experiments. A total of 10 fire spread experiments were not included in the analysis due to issues of quantifying key environment variables or due to significant changes in wind direction. Table 2 shows the distributions of the key variables used in the analysis per site.

Table 2. Mean (range), of weather characteristics, fuel structure and fuel moisture content and fire behaviour distributions per experimental site.

	Site				
Variables	Wangaratta	Ballarat	Tamworth	Toowoomba	Braidwood
Time of day (hh:mm)	11:32-15:30	10:13-15:20	11:50-16:00	10:20-16:10	10:00-19:30
Fire weather observations					
Air temperature (°C)	30 (27-33)	24 (16-32)	32 (29-33)	19 (18-21)	26 (17-37)
Relative Humidity (%)	18 (14-26)	34 (25-51)	36 (30-42)	47 (21-59)	33 (14-54)
Solar insolation (kW/m)	0.8 (0.2-1.3)	1.0 (0.9-1.1)	0.7 (0.4-1.0)	0.6 (0.2-0.8)	0.7 (0.1-1.4)
10-m open wind speed (km/h)	12.8 (6.2-20.0)	13.2 (3.6-25.8)	19.2 (12.6-25.7)	20.3 (7.8-35.7)	21.5 (12.9-45.3)
Grassland Fire Danger Index (GFDI)	2.9 (0.04 – 11)	4.0 (0.03 – 15)	5.5 (0.3 – 22)	4.5 (0.3 – 13)	11 (1.2 – 75)
Fuel structure					
Fuel bed depth (m)	0.58 (0.33 – 0.85	0.24 (0.18 – 0.29)	0.48 (0.29 – 0.57)	0.19 (0.16 – 0.25)	0. 23 (0.17 – 0.3)
Fuel load (kg/m^2)	0.42 (0.37 – 0.57)	0.32 (0.25 – 0.39)	0.27 (0.1 – 0.35)	0.33 (0.17 – 0.49)	0.25 (0.17 – 0.31)
Curing level (%)	67 (34 – 97)	77 (41 – 100)	69 (44 – 98)	84 (57 – 100)	91 (75 – 100)
Dead fuel moisture content (%)	5.9 (3.8-8.8)	7.4 (4.5-12.6)	6.1 (5.0-7.6)	8.8 (6.7-11.8)	8.8 (5.0-13.9)
Fire behaviour characteristics					
Rate of fire spread (m/min)	31.6 (3.3 – 85.7)	38.9 (2.8 – 102)	31.6 (8.7 – 58.1)	38.0 (6.9 – 92.3)	73.6 (21.6 – 150)
Fireline intensity (kW/m)	3769 (526-9342)	3725 (290-9670)	3420 (795-8834)	3467 (970-8370)	5161 (1840-11872)
Flame height (m)		1.9 (0.5 – 3.0)	1.3 (0.3 – 4.0)	1.3 (0.3 - 4.0)	1.8 (0.8 – 3.2)

Figure 10. Typical fire behaviour differences observed in a paired burn, Tamworth, NSW. Time since ignition: top image is 20 sec; middle image is 30 sec; bottom image is 40 sec. Images depict plot 5 (background; curing level 48%; sparse fuels) and plot 11 (foreground; 100% cured).

3.1.1. Fuel Structure and curing

Figure 11 shows the distribution of fuel height across the five sites. Observations range from 0.16 m (in Toowoomba) to 0.88 m (in Wangaratta). The Wangaratta site had the highest mean fuel height, 0.6 m, and widest range (0.33m – 0.88m). The Braidwood site had the lowest mean fuel height (0.23 m) and the smallest range, 0.17m to 0.31m. The largest proportion of fuel heights fell between 0.2 m and 0.3 m.

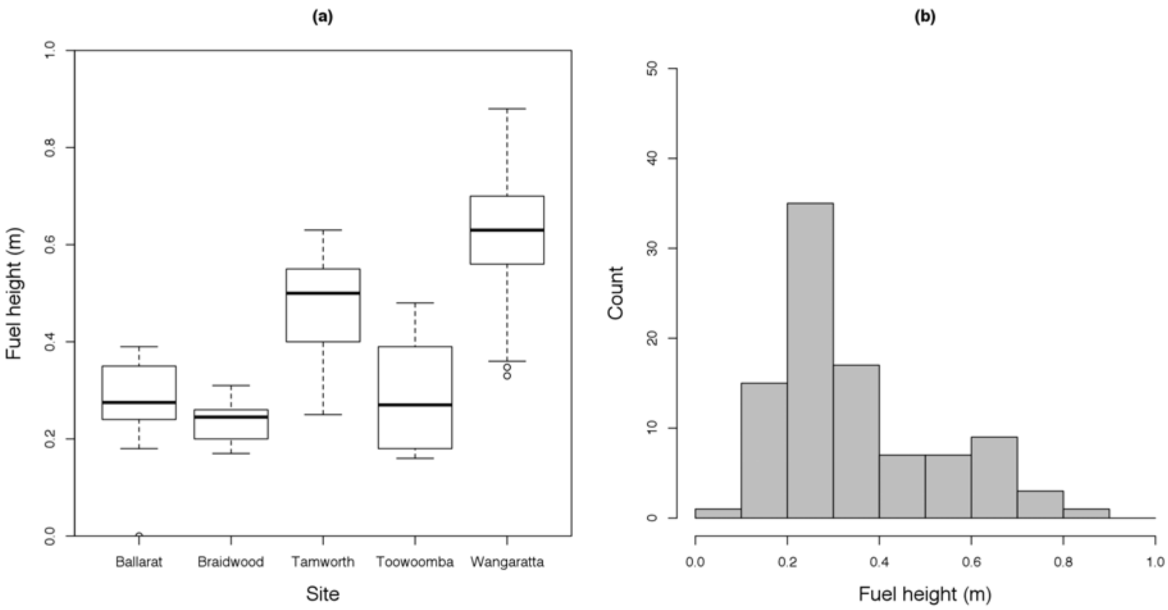

Figure 11. Boxplot and histogram describing the distribution of fuel bed height for the five experimental areas. Tick line in box indicates median. Box defines upper and lower quartile. Outer horizontal lines outside box reflect maximum and minimum values excluding outliers. Circles are outliers, defined as more than 3/2 times upper quartile.

Figure 12 shows the distribution of total fuel load across all sites. Total fuel load at the plot level ranged from a minimum of 0.17 kg/m^2 (in Toowoomba and Braidwood) to a 0.75 kg/m^2 (in Wangaratta). The Wangaratta site had the highest mean fuel load of 0.46 kg/m^2. The Braidwood site had the lowest mean fuel load (0.25 kg/m^2) and the smallest range of fuel loads, from 0.17 kg/m^2 to a high of 0.37 kg/m^2 (Figure 12). The Toowoomba site had the widest range of fuel loads (0.17 kg/m^2 – 0.50 kg/m^2) Fuel load show a distribution with a large concentration, 42% of data, within the range 0.2 kg/m^2 - 0.3 kg/m^2.

Plot level dead fuel load ranged from 0.11 kg/m^2 in Ballarat to 0.59 kg/m^2 in Tamworth (Figure 13). The highest mean dead fuel load (0.31 kg/m^2) was found at the Wangaratta site. The Toowoomba site had the widest range of dead fuel loads (0.14 kg/m^2 – 0.49 kg/m^2), although Tamworth had an 0.59 kg/m^2 outlier (Figure 13). The Braidwood site had the lowest mean dead fuel load (0.23 kg/m^2) and the smallest range of fuel loads (0.14 kg/m^2 – 0.32 kg/m^2). Notably, the average dead fuel load of 0.28 kg/m^2 found for the Wangaratta and Toowoomba sites was higher than the average overall fuel load of the Braidwood site (0.25 kg/m^2). This means that even though Braidwood had the highest curing values, the amount of dead fuel at the Wangaratta and Toowoomba site was greater than at the Braidwood site.

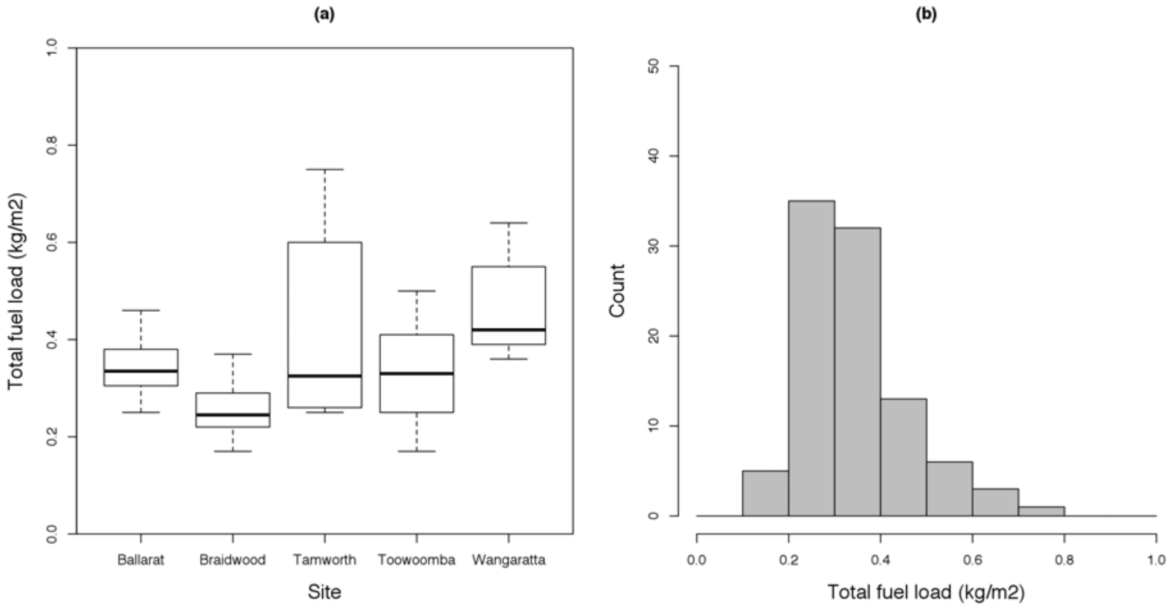

Figure 12. Boxplot and histogram describing the distribution of total fuel load for the five experimental areas. Tick line in box indicates median. Box defines upper and lower quartile. Outer horizontal lines outside box reflect maximum and minimum values excluding outliers. Circles are outliers, defined as more than 3/2 times upper quartile.

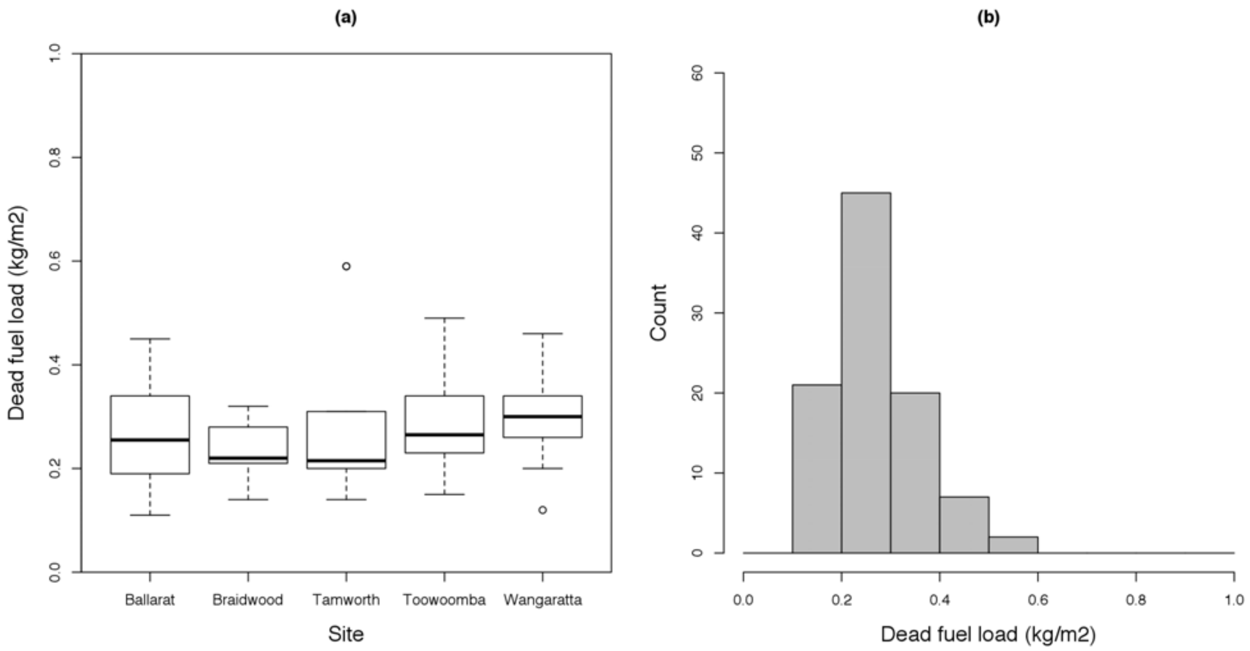

Figure 13. Boxplot and histogram describing the distribution of dead fuel load for the five experimental areas. Tick line in box indicates median. Box defines upper and lower quartile. Outer horizontal lines outside box reflect maximum and minimum values excluding outliers. Circles are outliers, defined as more than 3/2 times upper quartile.

Curing level was the key fuel variable controlled in this study. Considering the curing level distribution from non-herbicide treated plots, the dataset shows a good spread within the 40% to 90% range (Figure 14). Observations range from a low of 34% in Wangaratta to a high of 87% in Braidwood. The Wangaratta site captured the largest range of curing levels (34% to 84%). The Braidwood site captured the smallest range, 75% to 87%, with a focus on higher curing levels. The high values at Braidwood were due to the rapid progression of grass senesceence at this site, likely due to the predominance of very fine grasses, and a noted presence of substantial amount of fuel from the previous season. Tamworth and Ballarat had a substantial proportion of data below 60% curing.

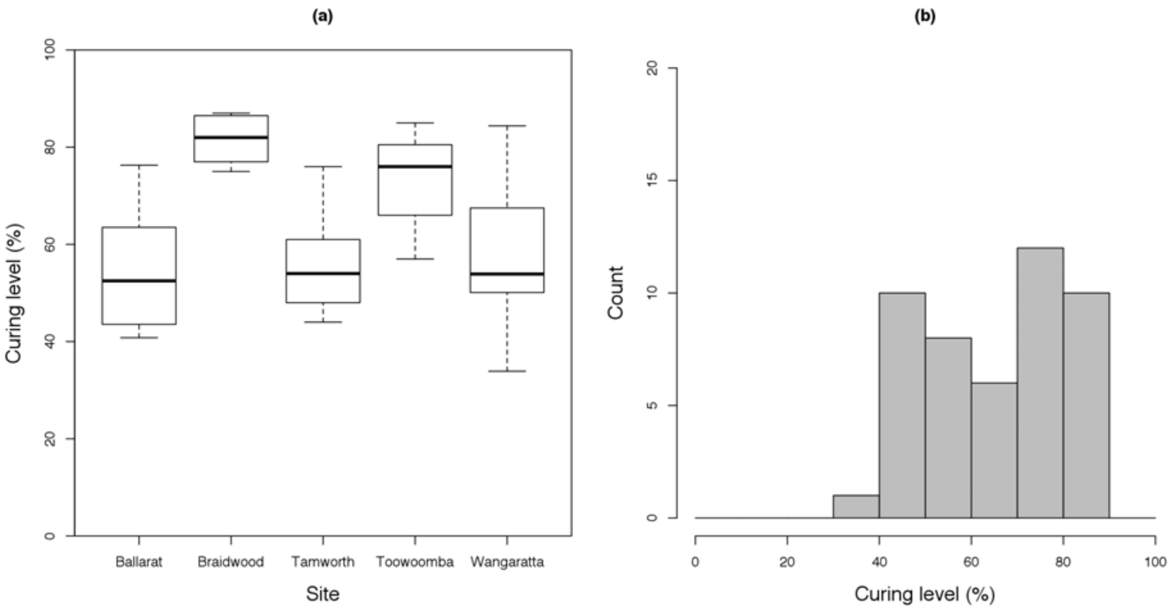

Figure 14. Boxplot and histogram describing the distribution of curing values sampled in the untreated plots for the five experimental areas. Tick line in box indicates median. Box defines upper and lower quartile. Outer horizontal lines outside box reflect maximum and minimum values excluding outliers.

Fuel bed bulk density (Figure 15), a measure of the compactness or density of the fuel bed, ranged from 0.43 kg/m^3 (in Wangaratta) to 2.56 kg/m^3 (in Toowoomba). The Toowoomba site had the highest average bulk density (1.29 kg/m^3) and captured the widest range of fuel bed bulk densities (0.70 kg/m^3 to 2.56 kg/m^3). The Wangaratta site had the lowest average fuel bulk density (0.82 kg/m^3) and the Wangaratta site captured the smallest range of fuel bulk densities (0.43 kg/m^3 to 0.98 kg/m^3). Fuel bulk density was more influenced by fuel height than fuel load, with the high fuel height values measured at Wangaratta and Tamworth contributing to the lowest fuel bulk densities at those sites.

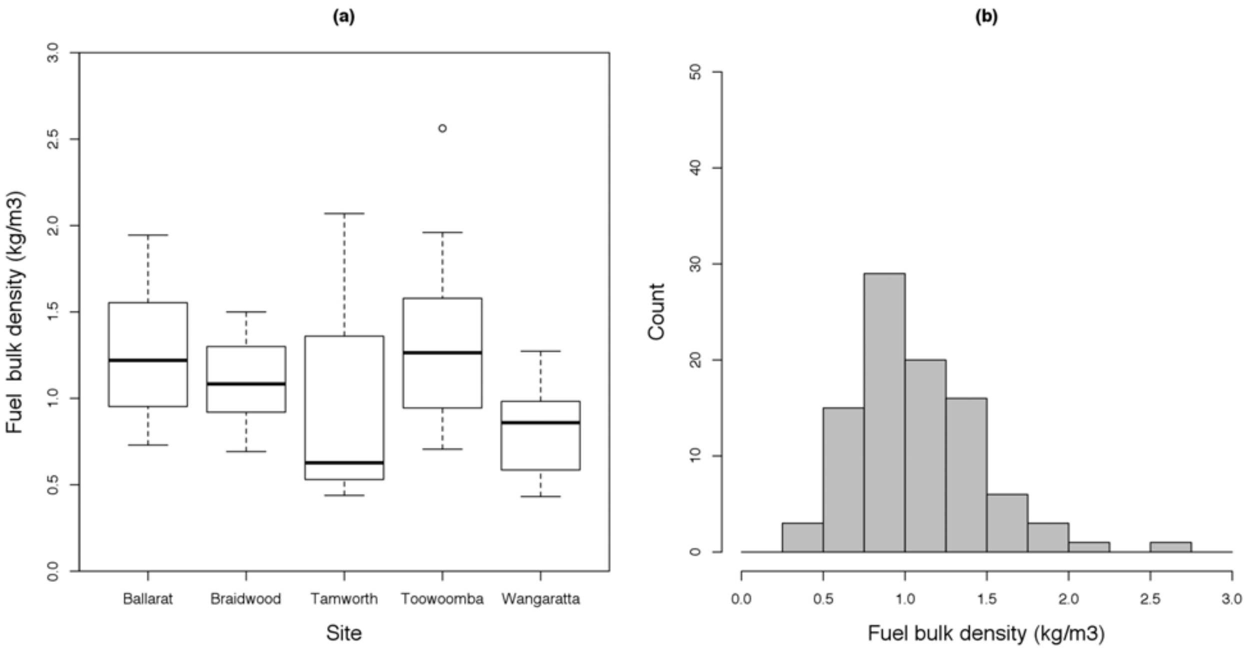

Figure 15. Boxplot and histogram describing the distribution of fuel bulk density for the five experimental areas. Tick line in box indicates median. Box defines upper and lower quartile. Outer horizontal lines outside box reflect maximum and minimum values excluding outliers. Circles are outliers, defined as more than 3/2 times upper quartile.

3.1.2. Fuel Moisture

Three fuel moisture content metrics were calculated: dead, live and overall. Figure 16 shows the distribution of dead fuel moisture contents across all sites. This variable range from 3.8% in Wangaratta to 13.9% in Braidwood. The lowest fuel moisture values were sampled within Wangaratta burns, with an average of 5.9% and a range of 3.8 – 8.8%. The Braidwood site had the highest mean, 8.8%, and the widest range 5 to 13.9%. The bulk of the dead fuel moistures were between 6% and 10%.

Figure 17 shows the distribution of live fuel moisture contents across all sites. Observations range from 17% (in Braidwood) to 120% (in Wangaratta). The Wangaratta site had the highest mean live fuel moisture content (90%) and the largest range of fuel heights (53% - 120%). The Braidwood site had the lowest average live fuel moisture contents (32%) and the Tamworth site had the smallest range of live fuel moisture contents (54% - 88%). These trends are linked to the range of curing levels and likely the fineness of the fuels. The distribution of live fuel moisture contents was relatively evenly distributed, with the majority of live fuel moistures between 60% and 100%.

Figure 18 shows the distribution of overall fuel moisture contents across all sites. Observations range from 5% (in Wangaratta, Wendouree and Braidwood) to 67% (in Wangaratta). The Wangaratta site had the highest mean overall fuel moisture content (34%) and the largest range of fuel heights (5% - 67%). The Braidwood site had the lowest average overall fuel moisture contents (12%) and the smallest range of overall fuel moisture contents (5% - 19%). These trends are strongly linked to the range of curing levels of the sites. The majority of the overall fuel moisture contents were between 5% and 15%.

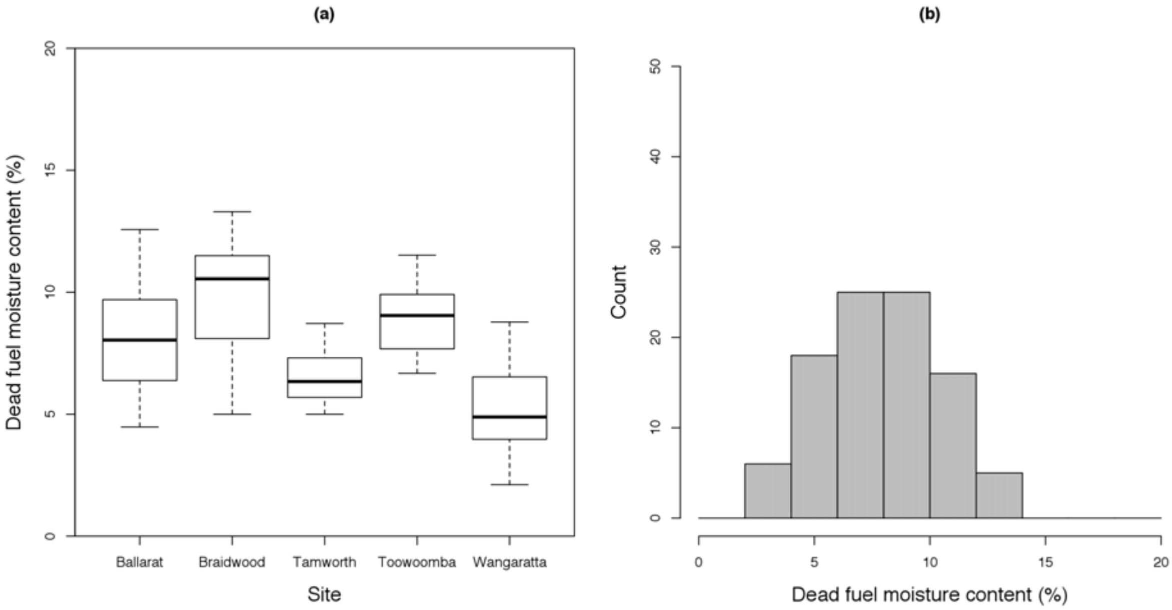

Figure 16. Boxplot and histogram describing the distribution of the dead fuel moisture content for the five experimental areas. Tick line in box indicates median. Box defines upper and lower quartile. Outer horizontal lines outside box reflect maximum and minimum values excluding outliers.

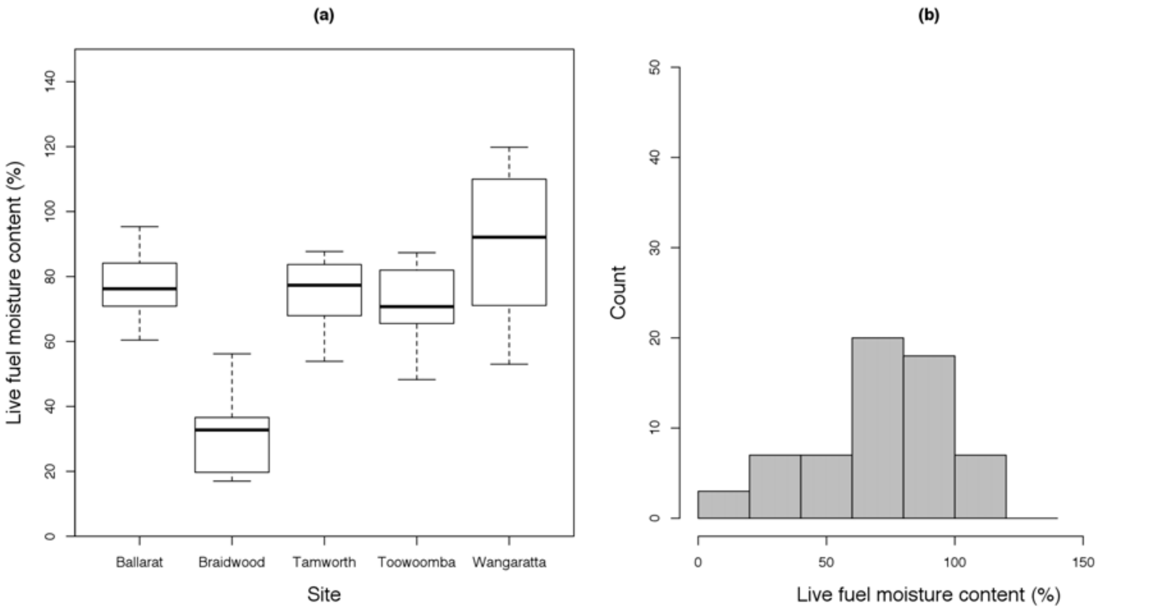

Figure 17. Boxplot and histogram describing the distribution of live fuel moisture content for the five experimental areas. Tick line in box indicates median. Box defines upper and lower quartile. Outer horizontal lines outside box reflect maximum and minimum values excluding outliers.

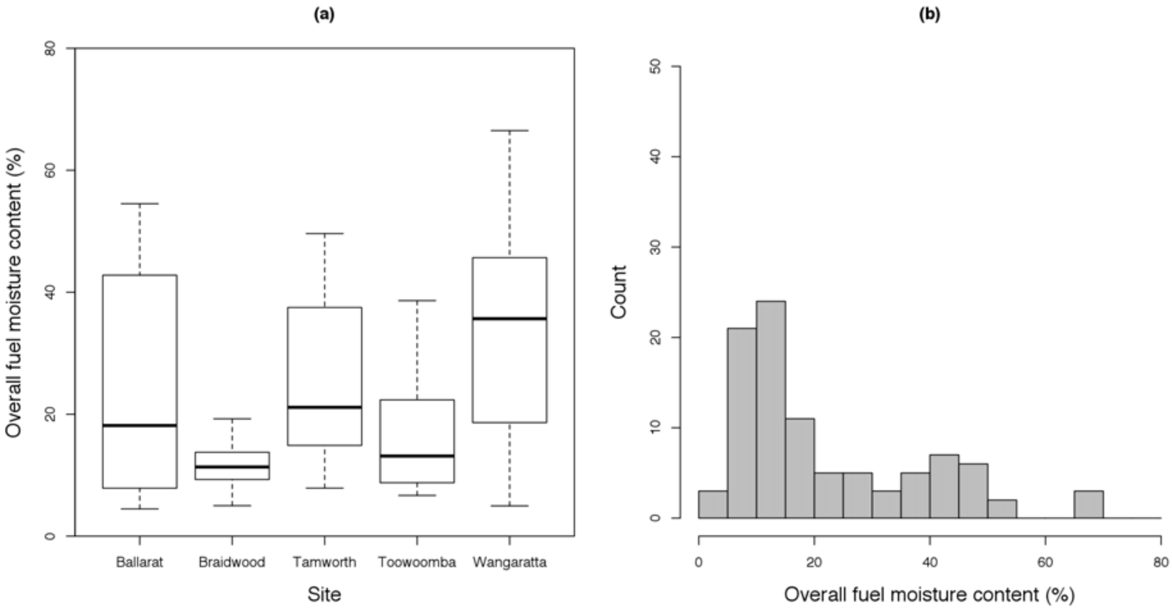

Figure 18. Boxplot and histogram describing the distribution of overall fuel moisture contents for the five experimental areas. Tick line in box indicates median. Box defines upper and lower quartile. Outer horizontal lines outside box reflect maximum and minimum. Circles are outliers, defined as more than 3/2 times upper quartile.

3.1.3. Wind speed and Grassland Fire Danger Index (GFDI)

10-m open wind speed varied between 3.6 and 45.3 km/h in the dataset. Wind speeds averaged around to 20 km/h for Tamworth, Braidwood and Toowoomba. Wind distribution at Wangaratta and Ballarat was characterized by lower wind speeds (Figure 19), averaging around 13 km/h. A small number of fires had average open wind speeds of less than 10 km/h, an indicator of light and variable winds. The maximum wind speeds under which fires were carried out were between 40 and 45 km/h (four of these experimental fires carried out at the Braidwood site). A total of four fires were conducted with winds higher than 40 km/h.

Figure 20 shows the per site distribution of Grassland Fire Danger Index (GFDI) assuming a 100% curing level. The highest GFDI values were observed at the Braidwood site, with a couple of experiments burned with a GFDI around 75. The Tamworth burns were also characterized by high GFDIs, albeit over a small range (4 to 22). Notably, the average GFDI for the Braidwood burns was more than double the average GFDI for the Wangaratta, Ballarat and Toowoomba sites. The differences in GFDI between these two groups were due mainly to the higher wind speeds in the high GFDI group. In particular, the average GFDI was lowest for the Wangaratta burns, GFDI = 4, despite this subset being also characterized by having the lowest dead fuel moisture contents.

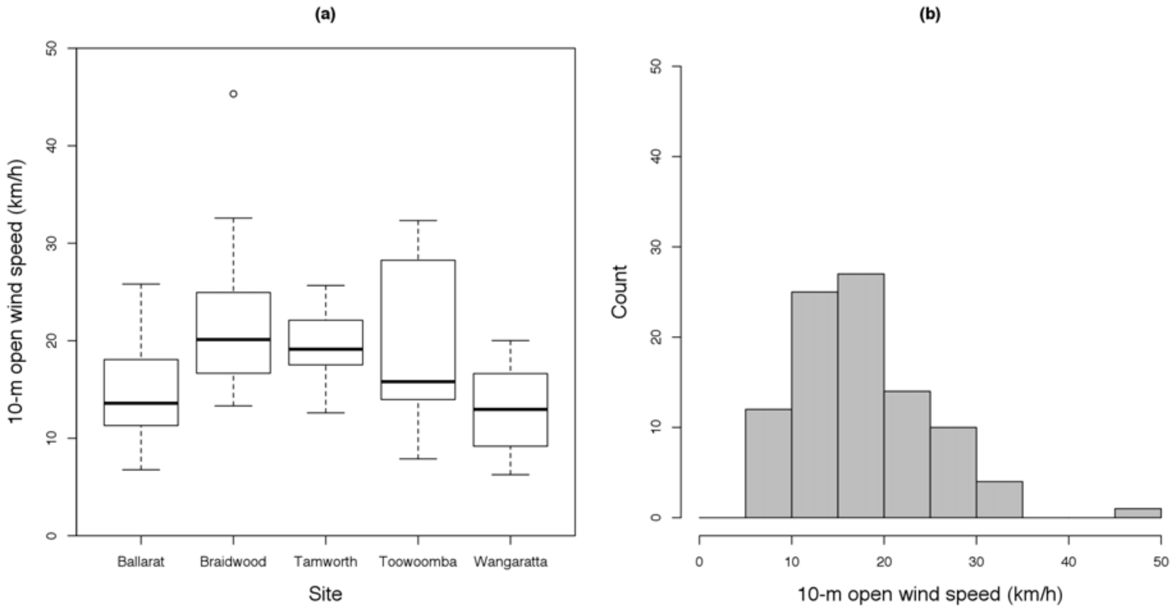

Figure 19. Boxplot and histogram describing the distribution of 10-m open wind speed for the five experimental areas. Tick line in box indicates median. Box defines upper and lower quartile. Outer horizontal lines outside box reflect maximum and minimum. Circles are outliers, defined as more than 3/2 times upper quartile.

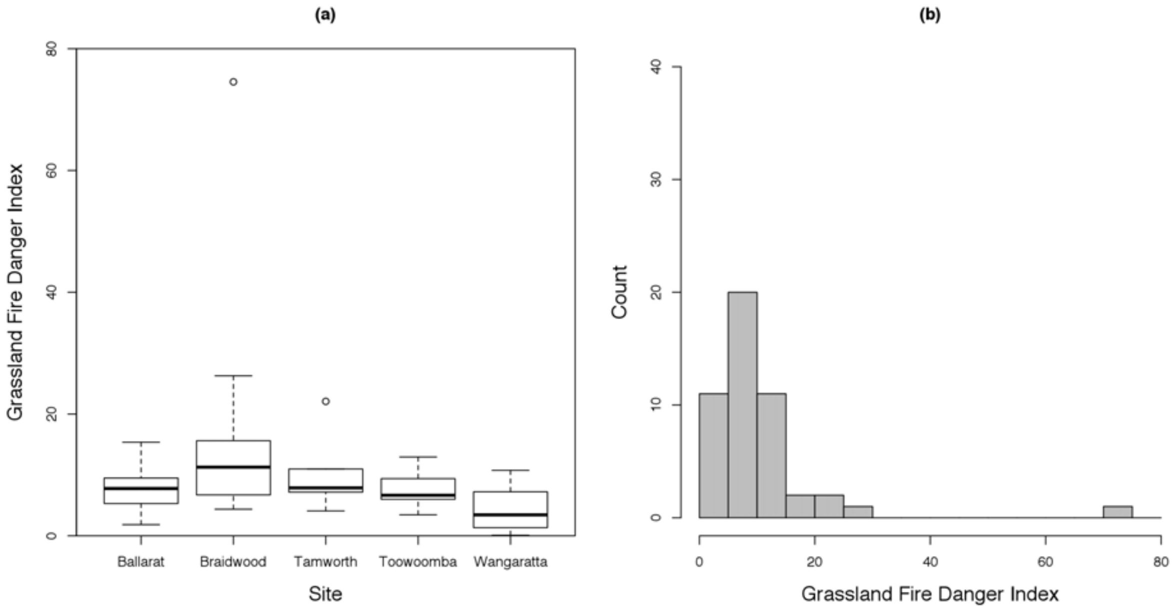

Figure 20. Boxplot and histogram describing the distribution of Grassland Fire Danger Index (GFDI) for the five experimental sites. GFDI depicted is restricted to full curing condition. Tick line in box indicates median. Box defines upper and lower quartile. Outer horizontal lines outside box reflect maximum and minimum. Circles are outliers, defined as more than 3/2 times upper quartile.

3.1.4. Fire spread behaviour

Figure 21 and Figure 22 presents the distribution of rate of fire spread obtained in fully cured and partially cured plots respectively for all five sites. Average rate of spread was 60.8 and 30.7 m/min, respectively for the fully cured and partially cured subsets. The Braidwood dataset showed the widest range in rate of spread in both fully cured and partially cured plots. This dataset had also the highest average rate of spread with an average of 82 m/min for fully cured plots and 63 m/min in partially cured plots. This difference between fully and partially cured conditions was the lowest of the 5 sites, owing to the high curing level of the partially cured plots, all above 75%. For the remaining sites, the average fire spread values of the fully cured plots were 2-3 times larger than the average rate of spread value of the partially cured plots.

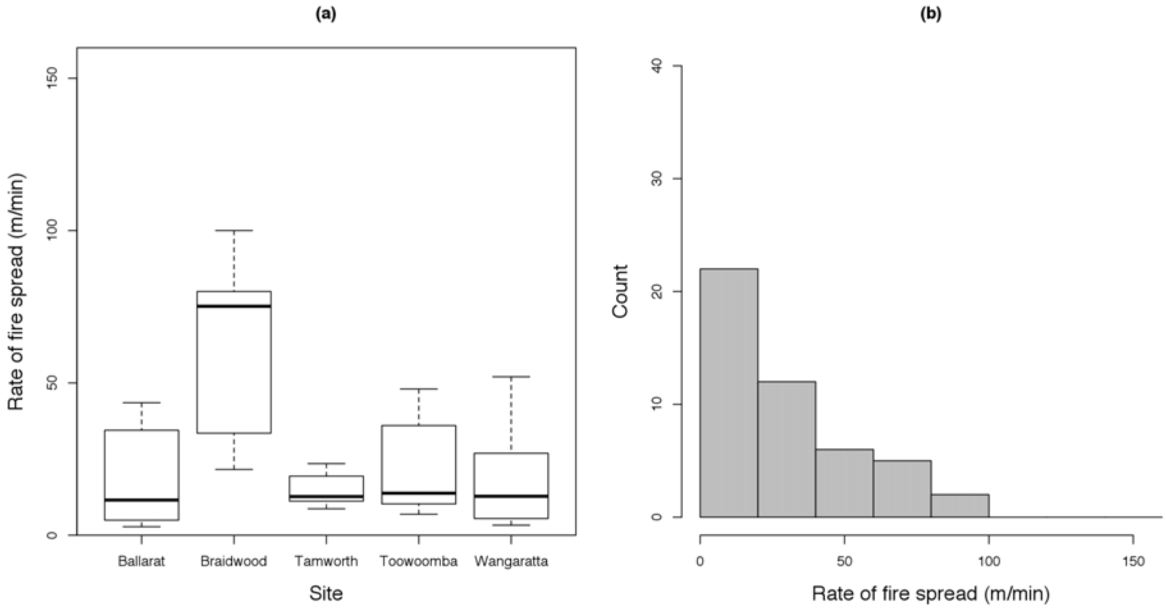

Figure 21. Boxplot and histogram describing the distribution of rate of fire spread for treatment (partially cured) fires. Tick line in box indicates median. Box defines upper and lower quartile. Outer horizontal lines outside box reflect maximum and minimum.

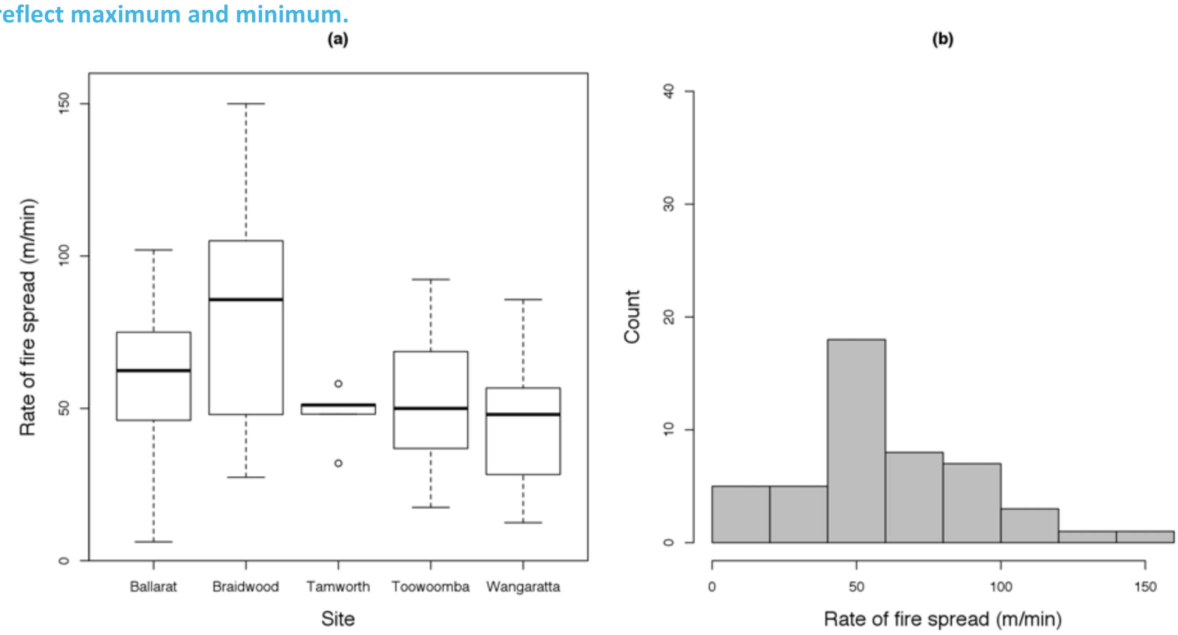

Figure 22. Boxplot and histogram describing the distribution of rate of fire spread for control (fully cured) fires. Tick line in box indicates median. Box defines upper and lower quartile. Outer horizontal lines outside box reflect maximum and minimum. Circles are outliers, defined as more than 3/2 times upper quartile.

Figure 23 shows the distribution of fireline intensities across all sites. Site average fireline intensities were calculated around 3500 kW/m for all sites except for Braidwood, where this value was close to 5200 kW/m. This was due to a combination of high wind speeds leading to fast spreading fires and high curing values in the treatment burns. The highest intensity burn was recorded at Braidwood in a fully cured plot (~12000 kW/m). The lowest calculated fireline intensity values were at Ballarat (minimum of 290 kW/m) and Wangaratta (minimum of 526 kW/m), corresponding to burns in very low curing grasslands.

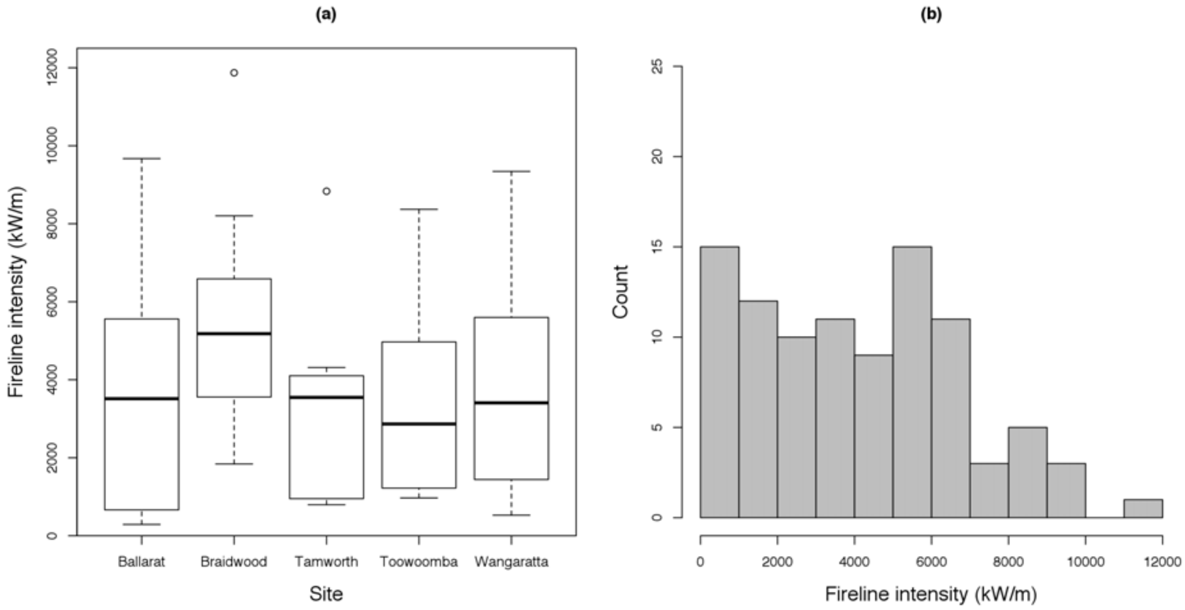

Figure 23. Boxplot and histogram describing the distribution of fireline intensity for the five experimental sites. Tick line in box indicates median. Box defines upper and lower quartile. Outer horizontal lines outside box reflect maximum and minimum. Circles are outliers, defined as more than 3/2 times upper quartile.

Figure 24 shows the distribution of flame heights from Ballarat, Braidwood and Toowoomba where reliable, validated flame heights were recorded (n=50). The range of flame heights were relatively evenly distributed across all three sites. The highest (4 m) and lowest recorded value (0.3 m) were both recorded at Toowoomba. Mean flame height was 1.9 m at Ballarat, 1.3 m at Toowoomba and 1.8 m at Braidwood.

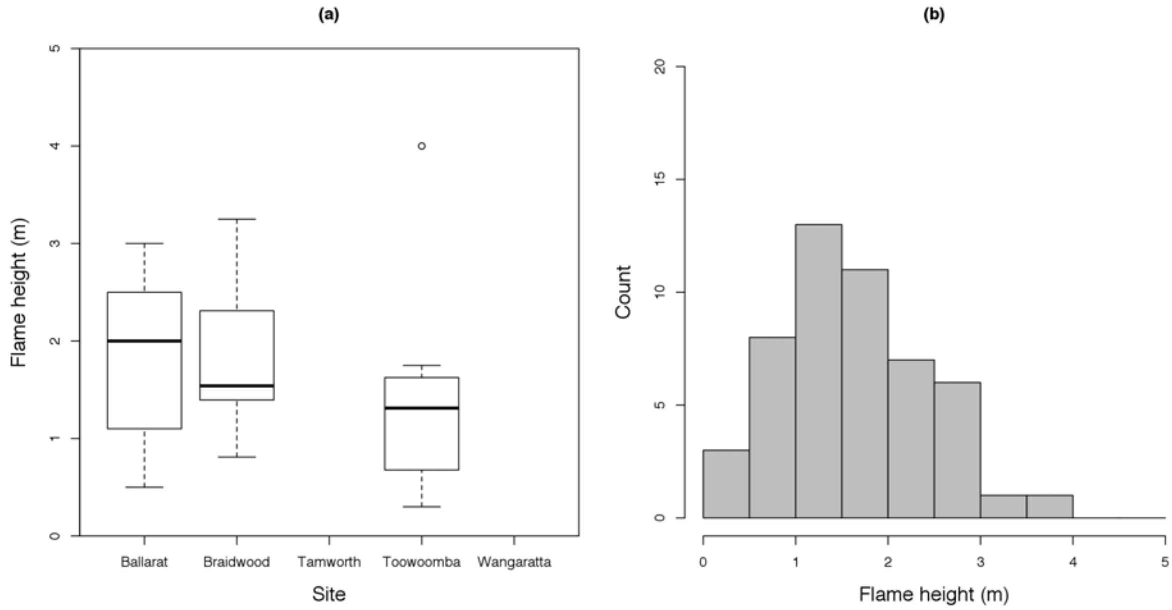

Figure 24. Boxplot and histogram describing the distribution of flame height for Ballarat, Braidwood and Toowoomba. Tick line in box indicates median. Box defines upper and lower quartile. Outer horizontal lines outside box reflect maximum and minimum. Circles are outliers, defined as more than 3/2 times upper quartile.

3.2. Fire spread sustainability

A total of 12 fire sustainability experiments were conducted. A group of six was conducted in Victoria and a further six in Tamworth. The Victorian burns had the lowest curing levels, between 21% and 30% (destructive sampling). All of the tests resulted in sustained fire propagation. At the Tamworth burns the curing levels yield values between 35% and 50%. Both sets of experiments were conducted under light and variable winds (2- m height wind speed lower than 6.5 km/h). Dead fuel moisture content varied between 5 and 6% in the Victorian burns and 6 and 8% in Tamworth. The moisture content of green fuels varied between 120 and 165%. All fires resulted in sustained fire propagation. The large quantity of smoke associated with these fires obscured observation of flame front dimensions. However, it was observed that the fire was able to spread by consuming the dead fuels at the base of each grass tussock. Post-fire assessments revealed that although the fires spread over 100% of the plot (i.e., no unburnt islands) with consumption of the dead fuels and senescing fuels, some of the green stalks remained unconsumed following the passage of the flame front.

3.3. Fire propagation experiments

3.3.1. Effect of curing on fire spread rate

The main aim of the evaluation of the published curing effect functions on rate of fire spread was to evaluate the equation developed by Cruz et al. (2015). This equation was developed with the data from the Wangaratta and Ballarat experimental fires, and the subsequent fires carried out in 2015, at Tamworth, Toowoomba and Braidwood, offered an opportunity to evaluate the equation against independent data. Table 3 provides the evaluation statistics for the Cruz et al. (2015) model against the original modelling dataset and the independent evaluation dataset (see also Figure 25). The evaluation statistics were found to be similar for the two datasets, notably, the mean absolute error is comparable (0.08 vs. 0.09) and there is an absence of bias for the evaluation dataset (MBE = 0.01).

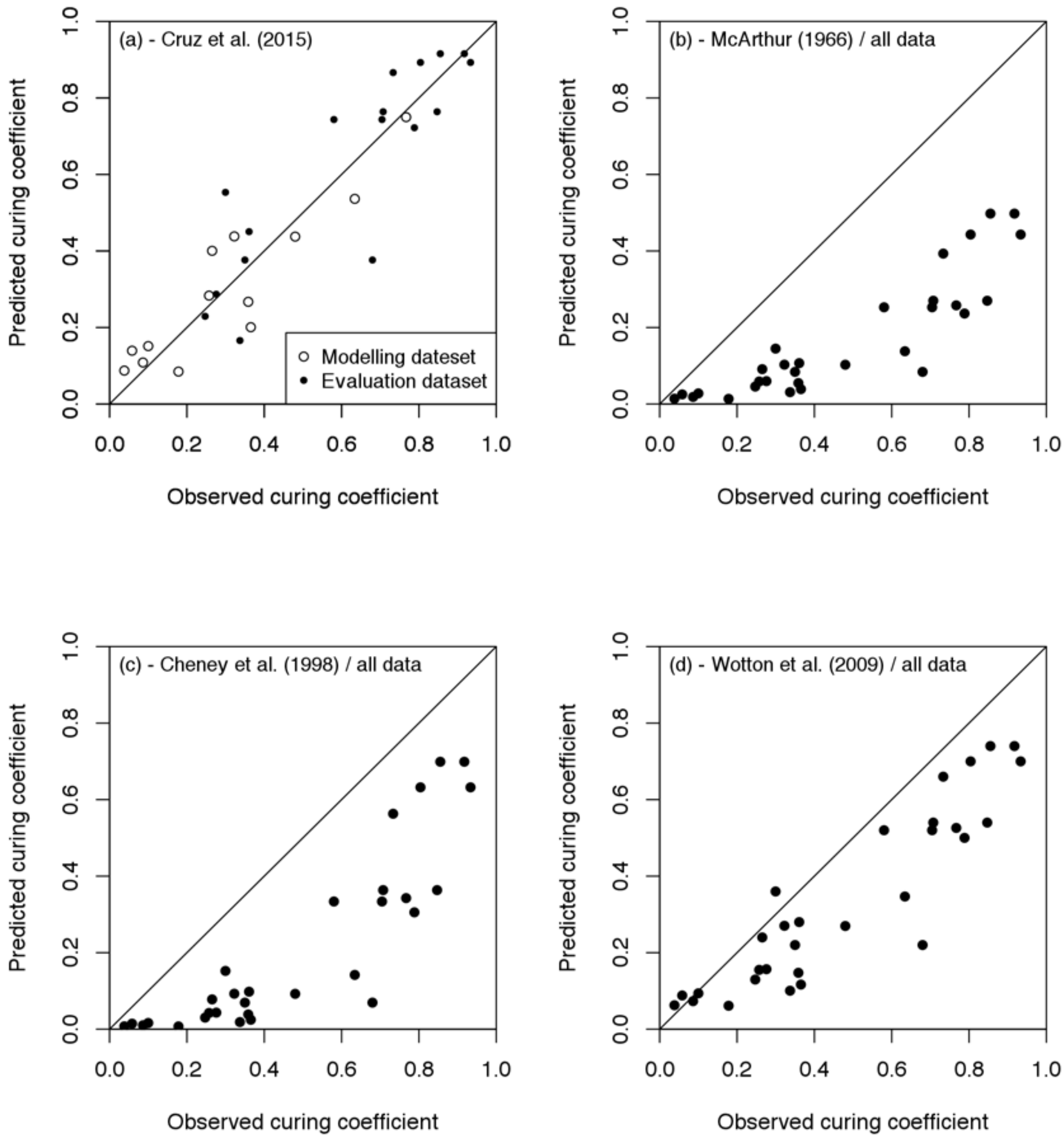

Figure 25. Observed vs. predicted curing coefficients for (a) Cruz et al. (2015), (b) McArthur (1966) GDFI/Mk 3, (c) Cheney et al. 1998, and (d) Wotton et al. (2009). Data for Cruz et al. (2015) is divided into modelling and evaluation datasets. All other models were evaluated with both datasets combined.

The Cheney et al. (1998) formulation yield an MAE of 0.27 and a MBE of -0.27, indicating an under-prediction trend, which would result in an under prediction of the potential rate of fire spread. Similarly, the Original Mk 3 formulation resulted in an MAE of 0.31 and a MBE of -0.31. The Wotton et al (2009) produced an MAE of 0.15 and MBE of -0.14.

Table 3. Error statistics for rate of fire spread curing functions tested. Note that the McArthur (1966) Mk 3 GFDI model is not currently used for fire spread prediction but only for grassland fire danger indexing/rating.

Models	RMSE	MAE (m/min)	MBE (m/min)	MAPE (%)
Cruz et al. (2015) (modelling subset)	0.09	0.08	0	46
Cruz et al. (2015) (evaluation subset)	0.13	0.09	0.01	19
Cheney et al. (1998)	0.3	0.27	-0.27	66
Wotton et al. (2009)	0.18	0.15	-0.14	35
Mk 3 GFDI	0.39	0.31	-0.31	66

3.3.2. Effect of curing on flame height

Curing level was only weekly related to the flame height ratio (r=0.18; p=0.39). Linear regression analysis showed curing level was not a significant predictor of the flame height ratio (p=0.391), explaining only 4% of the variation in the dependent variable.

Figure 26 shows the spread of the flame height ratios against the Cruz et al. (2015) rate of spread curing function. The results suggest that the effect of curing in flame height is less pronounced (i.e., curing causes a smaller reduction in the response variable) than observed for other fire behaviour metrics such as rate of fire spread (as illustrated by Cruz et al. (2015) function) and intensity. Further discussion on the effect of curing level on fire danger rating is given in Section 3.4.

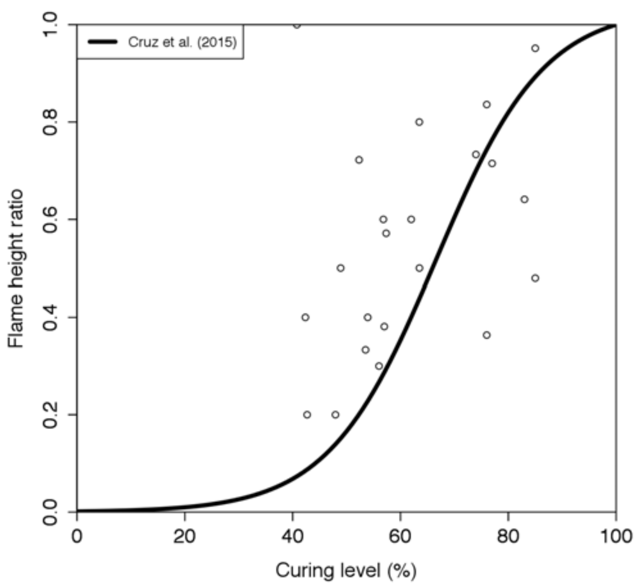

Figure 26. Relationship between the degree of grass curing and the flame height curing coefficient observed in experimental fires (filled circles) and the Cruz et al. (2015) rate of fire spread curing coefficient.

3.3.3. Effect of curing and fuel structure on residence time

Residence time was measured in 26 fires (20 in fully cured burns; 6 in partially cured burns). Table 4 shows the mean and ranges of residence time, environment and fire behaviour variables used in this analysis. There was no significant difference in residence time between fully (16.6 sec) and partially cured (16.5 sec) burns, for an overall average residence time of 16.6 sec. Considering the 26 fires, there was no significant correlation between residence time and any of the variables in Table 4, although Figure 27 suggests that some relationships might exist if a particular outlier was removed from the analysis. No significant relationships were found when the analysis was restricted to fully cured or partially cured condition.

Table 4. Statistical distributions of weather, fuel and fire behaviour variables used in the residence time analysis.

	Mean	St. dev.	Range
Residence time	16.6	7.6	7 – 44.4
2-m wind speed (km/h)	14.1	4.8	6.4 – 26.2
Dead fuel moisture (%)	7.1	2.7	3.5 – 12.6
Overall fuel moisture (%)	16.7	12.3	4.9 – 49.6
Curing level (%)	87.6	17.0	44 - 100
Dead fuel load (kg/m^2)	0.32	0.09	0.17 – 0.49
Total fuel load (kg/m^2)	0.38	0.12	0.17 – 0.68
Fuel bulk density (kg/m^3)	1.27	0.58	0.43 – 2.56
Rate of fire spread (m/min)	47.4	23.8	6.2 – 92.3
Fireline intensity (kW/m)	4956	2636	568 - 9670

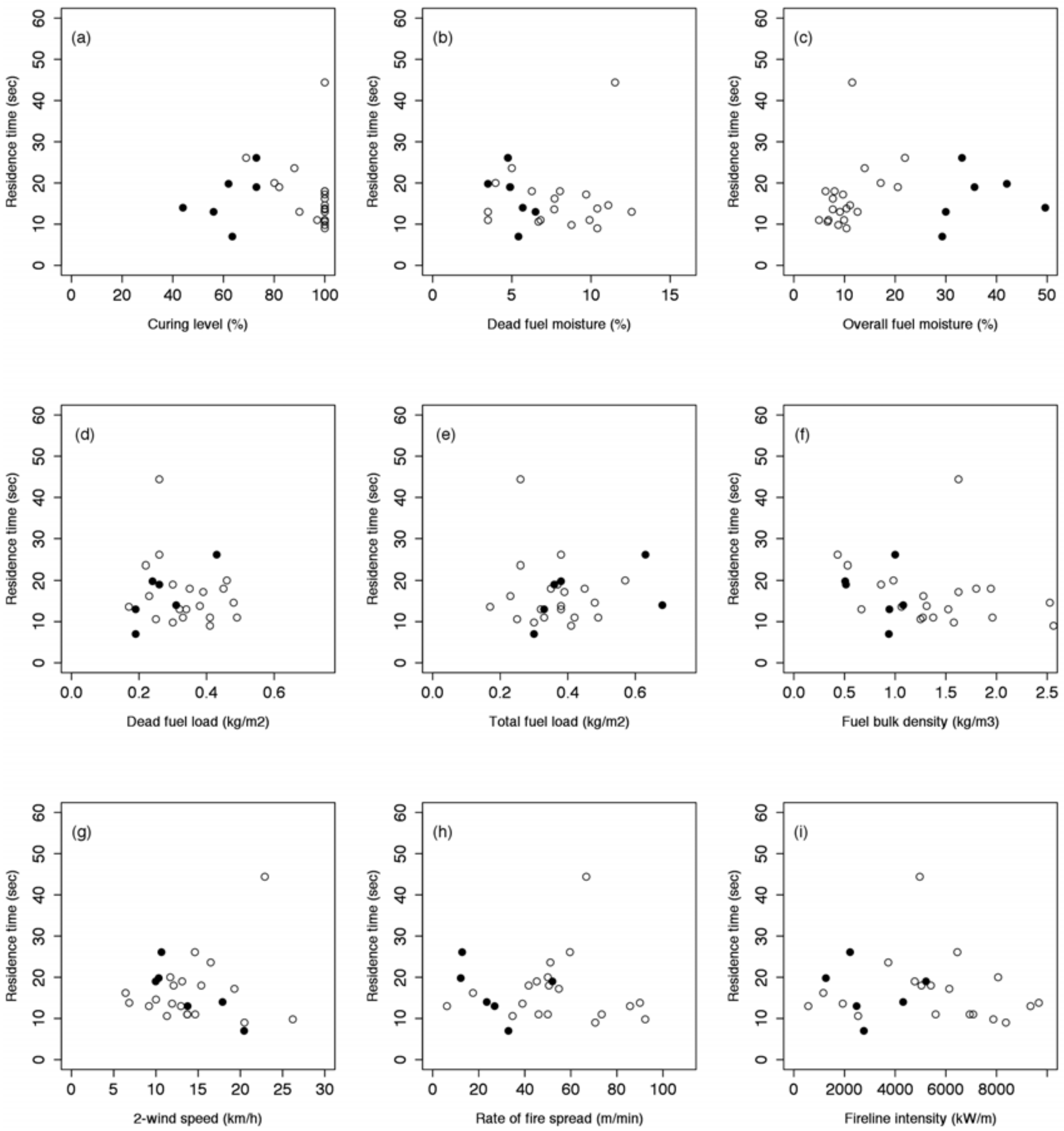

Figure 27. Scatterplots of residence time versus the major explanatory fire environment and behaviour variables analysed in the present study.

3.3.4. Effect of fuel load and structure on rate of fire spread and intensity

We aimed to analyse the effect of grass fuel load, bulk density and height on the rate of fire spread and intensity. We selected a subset of the dataset described in Section 3.1 where curing level was 100%. This constraint reduced the dataset to 33 fires, but allowed the study of the effect of fuel load and other structural characteristics without any confounding effects of curing. Table 5 provides basic statistics of the key fire environment and behaviour variables used in the analysis. This dataset includes the fastest rates of fire spread measured during the experimental burning program. Wind speed measured at 2-m height and dead fuel moisture content varied between 6.4 and 36.7 km/h and 4.5 to 12.6%, respectively.

Table 5. Statistical description (mean, standard deviation and range) of main weather, fuel and fire behaviour variables used in the fuel load and structure analysis (n=33).

Variable	mean	Stand. Deviation	range
U2 (km/h)	15.8	6.24	6.4 – 36.7
Dead FM (%)	9.0	2.33	4.5 – 12.6
Fuel load (kg/m^2)	0.29	0.08	0.17 – 0.49
Fuel height (m)	0.22	0.04	0.16 – 0.29
Fuel bulk density (kg/m^3)	1.34	0.37	0.84 – 2.56
Rate of spread (m/min)	67.4	53.0	6.2 – 150
Flame height (m)	2.0	0.71	0.9 – 3.25
Fireline intensity (kW/m)	5510	2660	567 - 11870

Table 6 provides correlation coefficients between the various variables. Wind speed was the only variable significantly correlated with rate of fire spread. Both dead fuel load and bulk density were inversely related with rate of fire spread, albeit not significantly (p= 0.32 and 0.15, respectively). Fuel load and height were significantly correlated (p<0.05) with fireline intensity. There was also a moderate correlation between these two variables, with a correlation coefficient of 0.313 (p=0.076).

Table 6. Pearson correlation coefficient, r, matrix for the fire environment and fire behaviour variables used in the fuel load and structure analysis (n = 33). Significant correlations (p<0.05) are shown in bold font.

	ros	Intensity	Flameh	u2	fuelDB	deadload	deadfm	fuelH
Ros	1	0.821	0.667	0.692	-0.251	-0.178	-0.154	0.150
intensity		1	0.691	0.480	0.172	0.372	-0.187	0.357
flameh			1	0.182	-0.186	0.110	-0.488	0.508
u2				1	0.013	-0.177	0.002	-0.259
fuelDB					1	0.782	-0.011	-0.315
deadload						1	-0.041	0.313
deadfm							1	0.028
fuelH								1

A model was created using non-linear regression analysis with 2-m wind speed and dead fuel moisture content in the form of Eqn 14. Wind speed was highly significant (p = 0.007), but dead fuel moisture content was not significant (p = 0.17). Despite being not significant for the current dataset, this variable was left in the model due to its relevance more generally. Residual analysis show both fuel load and bulk density to be clearly negatively related to the residuals, while there is a direct relationship between the residuals and fuel height (Figure 28).

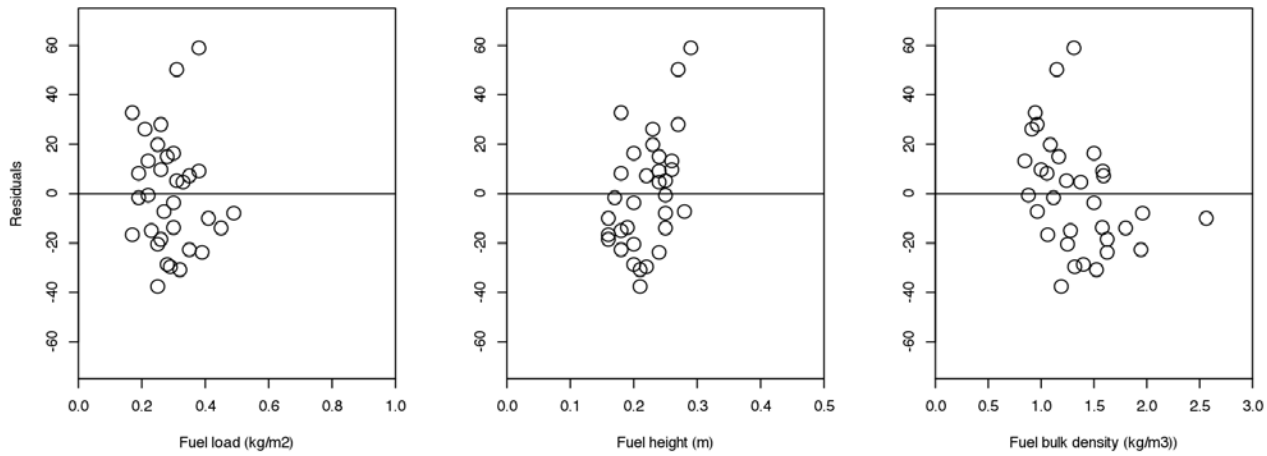

Figure 28.Scatterplots between residual rate of fire spread and fuel bed structural characteristics, (a) fuel load, (b) fuel height, and (c) fuel bulk density. The residual is calculated after modelling rate of spread from wind speed and dead fuel moisture content.

Adding fuel load to the model as a power function resulted in a non-significant (p=0.38) negative parameter (-0.21). Bulk density was a significant (p=0.02) variable in the model when entered as a power function, but noteworthy, with a negative effect (y=-0.56). The addition of bulk density also improved the significance of dead fuel moisture (p=0.11). Similarly, fuel bed height was found to be a significant variable when added to the model (y=0.67; p=0.51). The addition of this variable increased the significance of dead fuel moisture (p=0.10).

3.3.5. The effect of fuel load and structure on flame height

Flame height was significantly correlated with fireline intensity (r = 0.69), rate of fire spread (r=0.67), fuel height (r=0.51) and the moisture content of dead fuels. Flame height was not significantly correlated with fuel load (r=0.11; p=0.57). This lack of an effect of fuel load is also verified by the reduction in the correlation coefficient between flame height and (1) rate of fire spread and (2) intensity. We did not attempt to model flame height from our dataset, choosing to use our data to evaluate existent models (Section 3.3.6)

3.3.6. Evaluation of flame height models

The Cheney and Sullivan (1998) flame height model over predicted our observations (Figure 29a), with a MAE of 0.65 m and an MBE of 0.62 m. The differences between the observations and predictions (Figure 29b) are believed to be due to the different method used to measure flame heights in our study. Our method yield consistently lower values than visual estimates done during the experimental fires. Larger errors are observed for lower flame heights. Better fit was observed to occur for flame heights > 2.5 m.

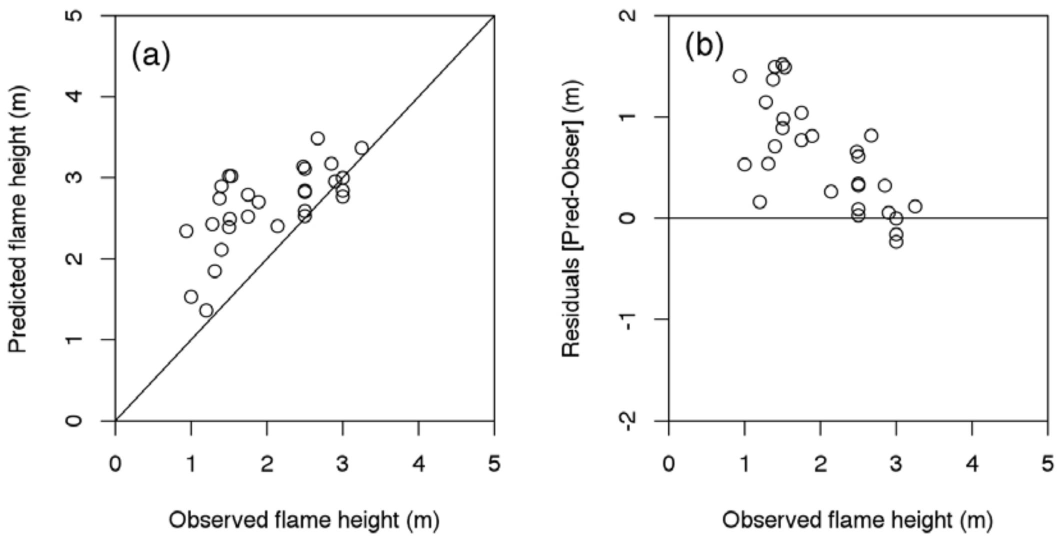

Figure 29. (a) Observed and predicted flame heights and (b) residual distribution with measured flame height.

3.5. Grassland Fire Danger Index (GFDI) and fuel structure

3.5.1. GFDI and grass curing

Figure 30 shows the effect of curing level in reducing the GFDI (from a full curing condition) and the respective control/treatment ratios for rate of fire spread (a); fireline intensity (b); and flame height (c). The results show that the curing function within the GFDI equation yields reductions in GFDI larger than observed for any of the fire behaviour quantities analysed (see Figure 31 for residuals distribution). The average error in the reduction in rate of fire spread was 0.33 (MBE=-0.33). Similarly the average error for the reduction in intensity was 0.37 (MBE=-0.33) and flame height was 0.49 (MBE=-0.48). The results show that the curing formulation in the GFDI results in a significant under estimation of fire potential for partially cured grasslands.

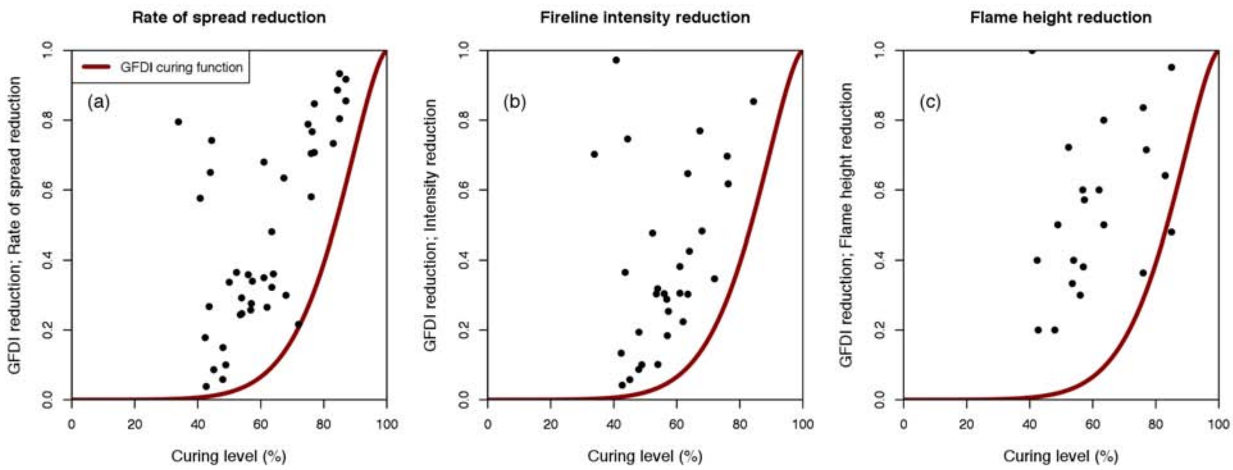

Figure 30. Relationship between the degree of grass curing and the Mk 3 GFDI reduction with the curing level effect in reducing (a) rate of fire spread; (b) fireline intensity, and (c) flame height.

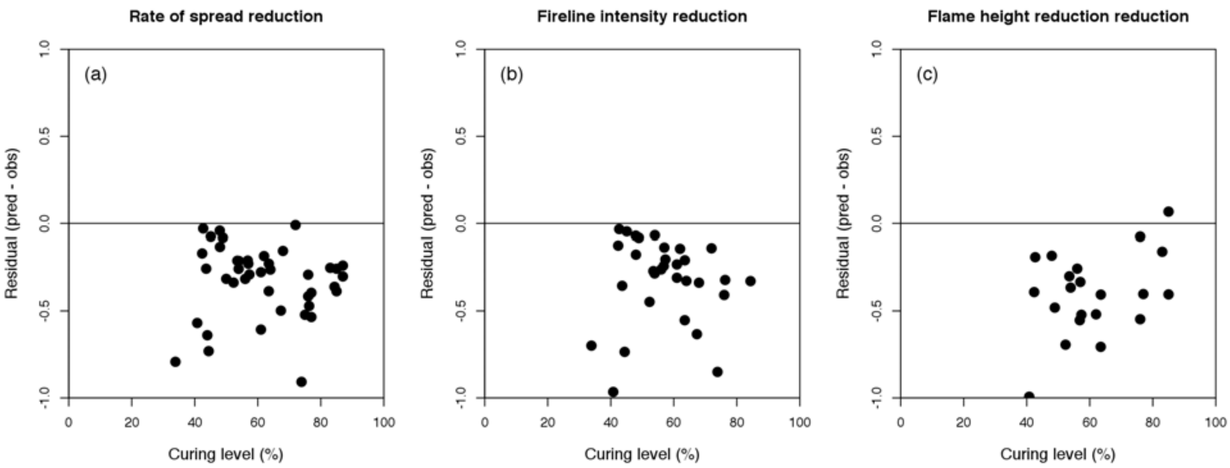

Figure 31. Residuals of GFDI reduction and observed reduction in (a) rate of fire spread; (b) fireline intensity, and (c) flame height.

Figure 32 further explores the relationship between the computed GFDI for each experimental fire and the fire behaviour quantities analysed. Figure 32a contrasts GFDI and rate of fire spread for fully and partially cured datasets. The vertical lines depict the fire danger rating class boundaries (Table 1). The horizontal lines represent corresponding boundaries in the rate of fire spread classes associated with each GFDI class (Table 1). Polygons with identifying letters inside (e.g., M, H and VH) have matching the GFDI and rate of spread class boundaries. Fires within such polygons have GFDI and rate of fire spread in the same class. Fires found in a polygon to the left of the identified polygons indicate a fire where the rate of spread was observed in the GFDI class immediately below the rate of spread class. The results show that although the fully cured data tend to be found on the identified polygons or on the polygon immediately to the left, the partially cured plots tend to be found two or three polygons to the left, meaning that their GFDI is two or three classes lower than the respective rate of spread class. This is noted for the faster fires in partially cured burns where rates of spread are higher than 43 m/min, e.g., a 100 m/min (6 km/h) spreading fire in the Moderate GFDI class.

Simple linear regression analysis through origin of rate of fire spread with GFDI as the regressor yielded a slope about 33% lower in the fully cured condition than found for the partially cured grasslands (Table 7). The 11.3 slope indicates that if grasses are partially cured, the current GFDI suggests an increase of 11.3 m/min per GFDI data point. For fully cured grasses the increase in spread rate per GFDI point is approximately 3.8 m/min.

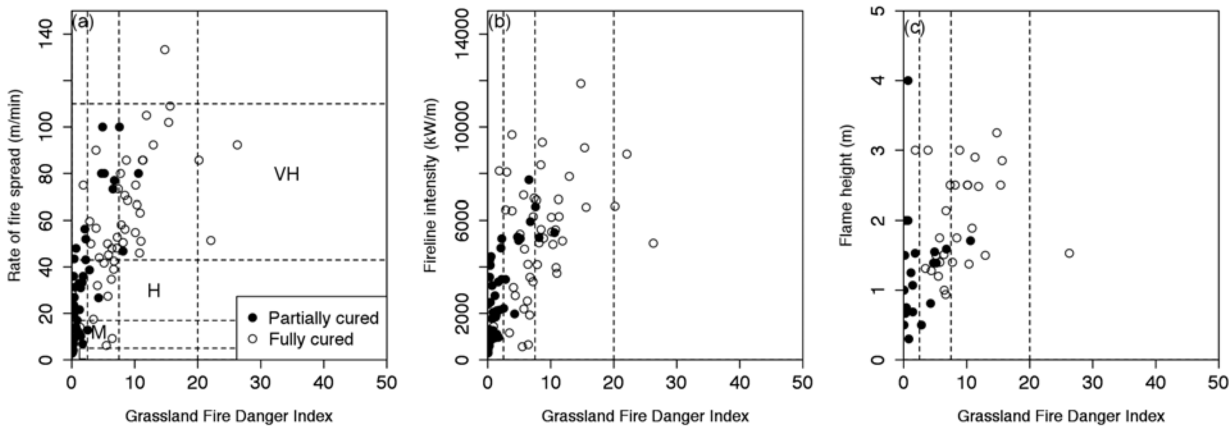

Figure 32. Distribution of fire behaviour observations by Grassland Fire Danger Index for partially cured and fully cured experiments; (a) rate of fire spread; (b) fireline intensity, and (c) flame height.

Table 7. Simple linear regression statistics of GFDI in rate of fire spread for fully cured (control) and partially cured (treatment) datasets.

	a	St. Error	P	R^2
Control	3.78	0.39	<0.001	0.66
Treatment	11.3	0.97	<0.001	0.76

Similar to what happened for rate of fire spread, Figure 32b and c shows that for a given fire behaviour level, as described by fireline intensity or flame height, the curing function in the GFDI formulation causes the partially cured data to occur at a lower GFDI value. Although there are fire danger rating classes that have been developed based on fireline intensity levels (e.g., Alexander and de Groot 1988; Alexander 2008), we chose not to plot them as per Figure 32a as such a definition would not be consistent with the original GFDI class definitions.

Linear regression analysis through origin of GFDI in fireline intensity yielded a slope about three times higher for the partially cured condition than for the fully cured condition (Table 8). Similar to what was computed for rate of fire spread as the response variable, the 883.6 slope indicates that if grasses are partially cured, the current GFDI suggests an increase of 883.6 kW/m per GFDI data point. For fully cured grasses the increase in intensity per GFDI point is 290 kW/m.

Similar analysis for the relationship of flame height and calculated GFDI for fully and partially cured burns yield comparable results (Table 9). The slope for the fully cured condition was 36% of the one calculated for partially cured grasses.

These results indicate that the curing formulation in GFDI is reducing the computed GFDI to levels not representative of the observed fire behaviour. This non representative reduction in fire behaviour is about one third than expected for the GFDI – fire potential relationship.

Table 8. Simple linear regression statistics of GFDI in fireline intensity for fully cured (control) and partially cured (treatment) datasets.

	a	St. Error	P	R^2
Control	290.0	42.0	<0.001	0.50
Treatment	883.6	84.8	<0.001	0.70

Table 9. Simple linear regression statistics of GFDI in flame height for fully cured (control) and partially cured (treatment) datasets.

	a	St. Error	P	R^2
Control	0.09	0.17	<0.001	0.46
Treatment	0.25	0.07	<0.001	0.36

3.5.2. GFDI and fuel load

In Section 3.3.4 and 3.3.5. we found fuel load to not have an effect on grassland fire rate of spread and flame height. In this section we extend the analysis to investigate the (1) effect of fuel load in improving the capability of GFDI to describe fire potential; and (2) the capacity of Purton's (1982) GFDI formulation to quantify fire potential. This analysis was based on the subset of fully cured experiments in order to remove the uncertainty associated with the effect of curing level and live fuel moisture content on fire behaviour.

Figure 33 depicts the relationship between GFDI and rate of spread with fuel load discretised by 3 broad classes (< 0.25 kg/m2; 0.251 to 0.4 kg/m2; > 0.41 kg/m2). The figure does not show an effect of fuel load on rate of fire spread. Multi linear regression analysis showed GFDI to be a significant predictor of rate of spread ($p<0.005$) and fuel load not ($p=0.744$).

Figure 33b shows fuel load to have an effect on fireline intensity, with the data from the lower fuel load class distributed below the middle and higher fuel load classes. This is not surprising as fireline intensity is directly proportional to fuel load. Multi linear regression analysis into fireline intensity had both GFDI and fuel load as significant explanatory variables ($p=0.001$ and <0.001, respectively).

Linear regression analysis of GFDI and fuel load in flame height showed both regressors to not be significant predictors of flame height ($p = 0.14$ and 0.28, respectively).

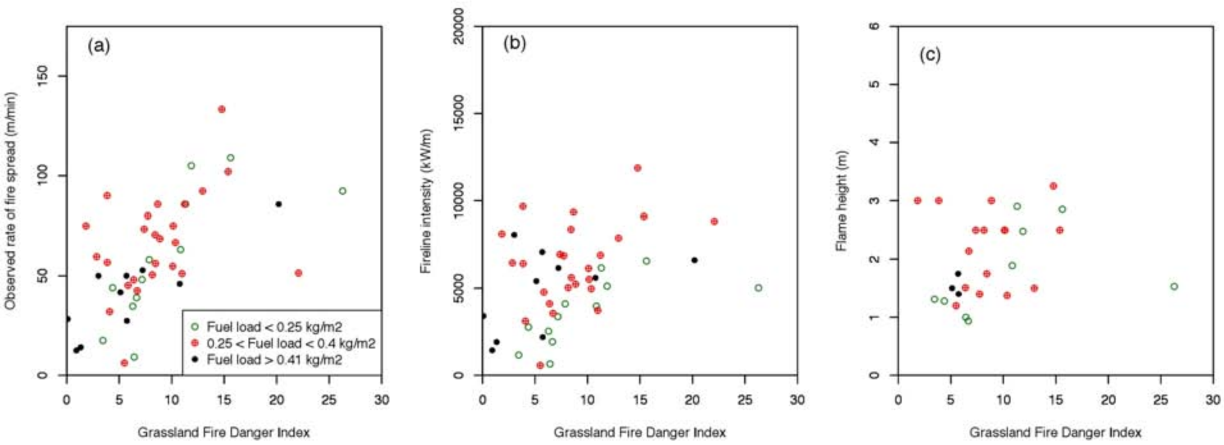

Figure 33. Relationship between grassland fuel load classes and fire behaviour observations with Grassland Fire Danger Index; (a) rate of fire spread; (b) fireline intensity, and (c) flame height.

The analysis of Purton's (1982) formulation with a fuel load effect in GFDI shows an overall reduction on the index value for the fully cured experiments. This results on a notable under prediction of fire potential. This is observed in Figure 34a. where most of the rate of fire spread data is located two fire danger index classes lower than the corresponding rate of spread class. It is also noted that using the Purton calculation, for a given GFDI the higher fuel load burns have lower rates of spread than the lower fuel loads. Similar to the rate of fire spread analysis, for fireline intensity, the use of the Purton GFDI results in most of the data between 7500 and 10000 kW/m to have a GFDI of 10 or less, a rather low number. It is worth noting that fire danger rating schemes based on fire intensity use the 10000 kW/m value as the threshold between Very High and the Extreme class (e.g., Alexander 2008).

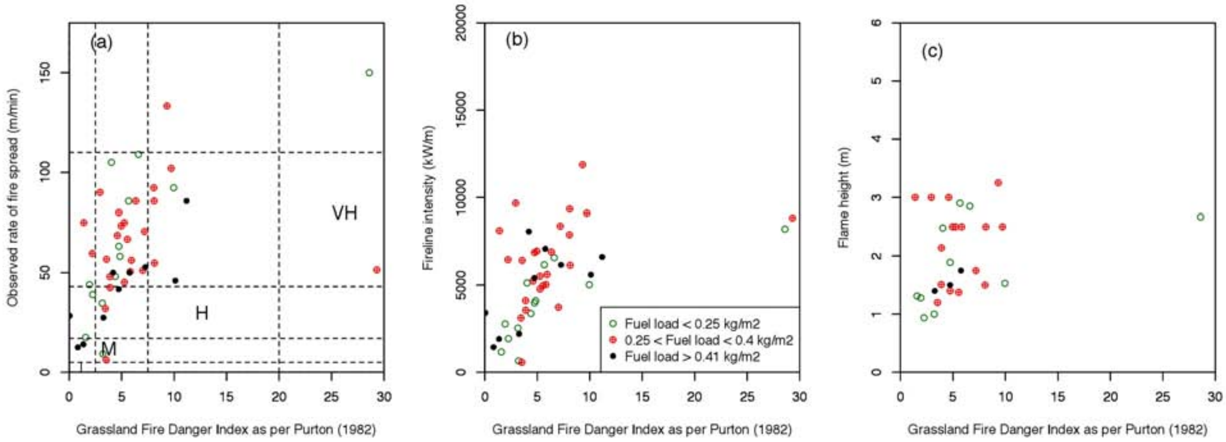

Figure 34. Relationship between grassland fuel load classes and fire behaviour observations with Purton (1981) Grassland Fire Danger Index; (a) rate of fire spread; (b) fireline intensity, and (c) flame height.

4 Discussion

Effect of curing on fire spread sustainability

Our results suggest that fires are likely to sustain combustion and active spread at curing levels lower than previously expected in Australia, where it has been commonly accepted that fires are unlikely to propagate at grass curing levels less than 50% (McArthur 1966; Cheney 1997; Cheney *et al.* 1998; Cheney and Sullivan 2008). We observed sustained propagation at curing levels between 21 and 30%, with dead fuel moisture content lower than 8%. It should be recognised that this curing threshold should also depend on the variables that determine heat transfer and the available energy for combustion, namely wind speed, dead and live fuel moisture and the amount of dead fuel (in our fires this variable was as low as 0.07 kg m^2.

For the lowest curing levels measured, approximately between 25 and 35%, it is important to recognise that propagation is marginal, characterised by a discontinuous flame front, low rates of spread and incomplete combustion (combustion was restricted to dead fuels and a small proportion of live ones). Nonetheless, this marginal combustion might be enough to maintain landscape fuel continuity, e.g., connecting areas of forest separate by grasslands, during periods of high forest fire potential but low grassland fire danger. Conversely, in open grasslands, if the landscape level curing assessment is characterized by such level of curing, it is likely the fire will self-extinguish when encountering localised areas of lower curing, such as close to creek lines or where soils and topography allow higher soil moisture content to be maintained.

Effect of curing on fire behaviour

Our analysis on the effect of curing on fire behaviour considered three fire behaviour characteristics: rate of fire spread, fireline intensity and flame height.

Relative to the effect of curing on rate of fire spread, our analysis focused on evaluating the function developed by Cruz et al. (2015), based on the Wangaratta and Ballarat subsets of data, and extend the evaluation of previously developed functions with the full study dataset.

The evaluation of the Cruz et al (2015) function yielded very encouraging results relative to its validity outside the bound of its original dataset. In particular, there had been concerns about the soundness of the model at upper curing levels and in grasslands with different physiological structures, namely for lower and higher fuel loads. The Tamworth, Toowoomba and Braidwood datasets allowed the evaluation of the Cruz et al. (2015) function for these conditions. The error statistics computed for this evaluation dataset were comparable to the ones obtained with the development dataset, substantiating the validity of the model in common grasslands found in Southern and Eastern Australia.

The evaluation of the McArthur (1966), Cheney *et al.* (1998) and Wotton et al. (2009) curing functions showed these to result in a under-prediction bias of fire spread rate potential in southern Australian pastures. This under prediction bias was found not to be trivial. Comparison between the damping effect of the Cruz et al. (2015) function and those of McArthur (1966) and Cheney *et al.* (1998) showed that the new function will predict fire spread rates to be approximately 10 to 2 times faster at degree of curing levels between 50 and 80% (Fig. 34).

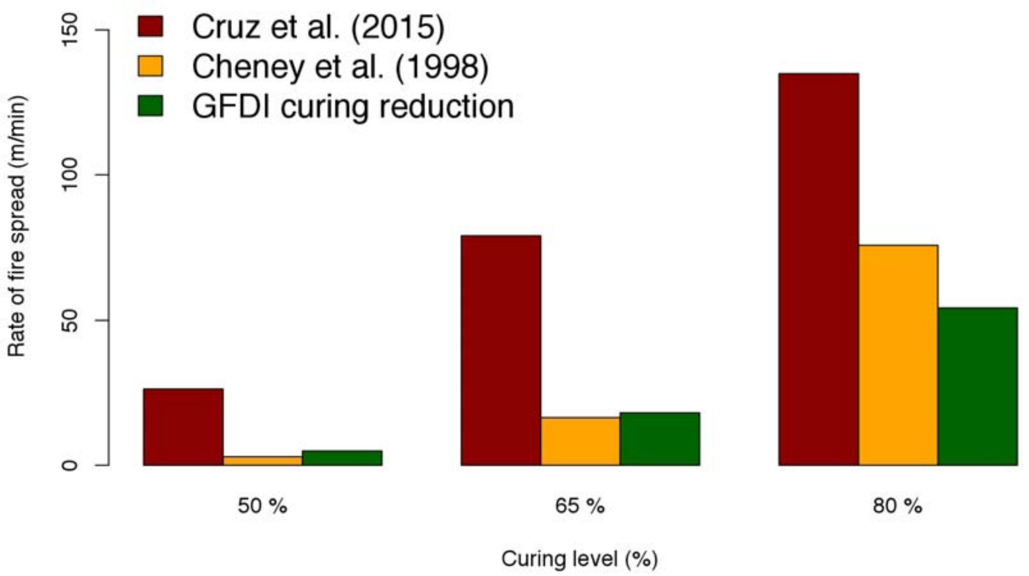

Figure 35. Comparison between predicted rates of fire spread with distinct curing levels for the Cruz et al. (20015), Cheney et al. (1998) and the McArthur (1966, 1973) Mk 3/4 Grassland Fire Danger Index (GFDI) curing coefficient functions Simulations consider a potential rate of fire spread for fully cured grasslands of 164 m/min as determined by the following environmental conditions: air temperature = 35 °C; relative humidity = 10%; and 10-m open wind speed = 35 km/h.

The Cruz et al. (2015) curing function is based on the assumption that the bulk curing effect is a surrogate for the effect of the amount of dead fuel in the fuel bed and the overall fuel moisture content. The main advantage is its simplicity (i.e. only estimates of degree of curing are needed) and the potential to be immediately implemented in current fire danger rating and fire behaviour prediction systems that rely on the degree of curing as an input.

One perceived disadvantage is that this function does not provide insight into how the live fuel load (or proportion) and moisture content influence the fire spread mechanisms at a more fundamental level. The application of a more detailed analysis of the energy requirements for ignition and fire spread as done by Catchpole and Catchpole (1991) would require knowledge of the amount of live fuel and its moisture content at any one time during the fire season. The use of such an approach would void the applicability of the current modelling results as those two quantities are currently not systematically sampled, either in Australia or anywhere else for that matter. Accurately estimating live fuel quantity is a complex exercise (Kidnie *et al.* 2015) and fraught with error (Andrews *et al.* 2006).

The present study focused on the effect of the degree of curing in senescing grasslands. During this process, fuels categorized as 'live' range from fully functional green plant components to senescing plant parts with fuel moisture contents around 60-80% (Luke and McArthur 1978). Changes in the degree of curing due to new plant growth, which occurs occasionally in Australia after significant mid-summer rains that cause annual grasses to resprout or perennial grasses to reshoot, resulting in a distinctly different fuel complex where all the live fuels have very high fuel moisture contents. As such, for the same level of curing, the average moisture content for live fuels in the regrowth scenario will be higher then found generally for senescing grasslands. Similarly, for the same curing level, the overall fuel moisture will be higher in the regrowth situation than during the grassland senescence.

The effect of this regrowth on fire behaviour seems to depend on the overall grassland fuel structure. In the experimental fires carried out by Cheney *et al*. (1993, 1998), the visually assessed curing level from regrowth varied between 85 and 95% and showed a negligible effect on rate of fire spread. This negligible effect might arise from the relatively tall and dense grasslands where the burns were conducted. The regrowth was distributed close to the soil, whereas the cured grasses formed a canopy layer that sustained fire propagation without a damping effect of the green materials underneath. We conducted a number of regrowth burns (not described in this report) at the Braidwood site, where the rate of spread was dampened to slower spread rates/intensity than observed for a similar curing level in a senessing grassland. We believe that the low fire potential observed in these burns arose from the combination of low fuel load, low height and well intermingled dead and live fuels, the latter with high fuel moisture content (between 150% and 200%). These factors could explain the lower flammability of this fuel complex when compared with a senescing grassland.

Our study focused on temperate eastern and southern Australia pastures. It is unknown how applicable the present results are to structurally very different grassland fuels, such as some tropical and sub-tropical grasslands (Rowell and Cheney 1979), invasive species or semi-arid grasses. Fuel loads in coarse thick-stemmed perennial grasses of the tropics and subtropics can be much higher than found in southern Australia temperate pastures. Such high dead fuel loads could support high intensity fire propagation even under low curing levels. Fire dynamics, and in particular the effect of curing in these grasslands, might be characterized by a different curing function than that found for southern Australia temperate grasslands (Luke and McArthur 1978, page 117). As an extreme example, sugar cane plantations burned prior to harvest have typically only 20% dead fuel but sustain high intensity fire propagation even under mild burning conditions (Cheney and Just 1974). Stands of invasive gamba grass (*Andropogon gayanus*) in Northern Australia attain similar fuel structures and comparable fire dynamics might be expected.

Similarly, certain semi-arid grasslands, such as hummock spinifex grasslands, also show recognizably different growth form and fuel distribution (Burrows *et al.* 1991, 2009) than the grasses used in our study. Fuel accumulation and moisture content dynamics in spinifex grasslands are quite different from the ones used in our study. It is not expected that the function developed in the present study will have validity for spinifex grass fuel complexes.

While annual grasslands go through the senescing process, there is a significant spatial variation in curing at the landscape level. Typically grasses on ridgelines will fully cure before grasses in lower elevations, such as along creek lines and depressions (Cheney 1997). The impact of this spatial variation of curing on fire growth is unclear but is expected to reduce the overall rate of spread of landscape fires.

Flame dimensions reflect the rate of energy released by a fire. Flame size is related to the rate of fire spread. As the rate of energy released per unit area of the flame front (i.e., fire intensity) is increased due to faster rate of spread or a higher quantity of fuel being volatilised in the flaming front, resulting in increased flame volume. The transient nature of flames makes them an elusive parameter to quantify and of poor scientific or engineering value (Rothermel 1991). Nonetheless, our ability to visualise the general dimensions of flame (height, angle and length) makes a simple and efficient method to qualitatively assess fire intensity. This allows practitioners to link fire behaviour with efficiency of suppression methods and tactics, but it should be understood that flame height and length measurements are fraught with uncertainty.

There was a lack of correlation between flame height ratio (Eq. 8) and curing level. This was likely due to the interaction of other variables controlling flame height - such as wind speed, available fuel load, dead fuel moisture content and rate of spread/intensity; and errors in estimating flame height. Nonetheless, the calculated flame height ratios followed the Cruz et al. (2015) rate of spread curing function, albeit with a less pronounced effect.

Effect of fuel load on fire behaviour

The fire behaviour dataset gathered in our study offered a unique opportunity to investigate the effect of grass fuel load on fire behaviour. The analysis showed an inverse relationship between grass fuel load and rate of fire spread, albeit not a significant one. No significant correlation existed between fuel load and wind speed and fine dead fuel moisture, clearing any possible auto-correlation issues that could influence the fuel load – rate of fire spread relationship. After taking into account the effect of wind and dead fuel moisture content on rate of fire spread, fuel load was still inversely and non-significantly related with rate of fire spread.

Our results are comparable to those found by Cheney et al. (1993) in northern Australia grasslands, namely in *Eriachne burkittii* R. Br. (known locally as kerosene grass) and *Themeda australis* R. Br. (kangaroo grass). These experiments were conducted with the purpose to "*determine the relative importance of fuel characteristics on fire spread and in particular to resolve the conflicting information about the importance of fuel load*" Cheney et al (1993). Despite the wide range in fuel loads, 0.02 to 0.57 kg/m2, "*no evidence that fuel load had a direct influence on spread rate*" was found. Although fuel bed height and bulk density were significantly correlated with rate of fire spread.

Flame height is determined by the interaction between the horizontal momentum of the local wind and the vertical buoyancy forces generated by the energy released by the fire (Albini 1981). Wind speed also influences flame height by indirectly determining the buoyancy forces, through its effect on the rate of fire spread and intensity. Although useful for suppression planning, grassland flame heights are known to be relatively small when compared with similar intensity fires in other fuel types, such as in forest or shrublands (Cheney 1990). Even in exceedingly fast grass fires, flame heights tend to not increase beyond 4 to 5 m tall.

We did not find a relationship between flame height and dead fuel load in grasslands. The lack relationship is likely the result of the relative small range of fuel loads observed in Southern Australia grasslands (2 – 6 t/ha), the small residence time for these fuels, and the above mentioned effect of wind speed, which counter acts the vertical buoyant forces. Although these results seem to hold well in Southern Australia grasslands, it is unclear if the same relationship will be maintained for higher fuel loads, namely around 1 kg/m^2, that have been reported in certain grass types, such as some exotic grasses.

Evaluation of the GFDI curing function – Implications to fire danger rating

The current curing function implemented in the Grassland Fire Danger Meter (GFDI) currently used in Australia imposes a stronger damping effect on rate of fire spread, fireline intensity and flame heights than observed in our datasets. The current GFDI damping effect for partially cured grasslands results in an under prediction of fire potential by a factor of three.

The significant under estimation is particularly relevant for occasional periods of high wind speed paired with low relative humidity's occurring prior to full curing. The current formulation will suggest abated levels of fire behaviour while evidence indicates very high to extreme levels of fire behaviour might occur. From a fire-fighter point of view, this under prediction bias can result in non-recognizing the full fire potential, leading to possible life threatening situations.

Should the curing coefficient function in the GFDI equation be changed to incorporate the findings from the present study? The answer to this question is not as simple as it appears. The GFDI and associated fire danger classes have been used in Australia for nearly 50 years to support a number of fire management activities, such as to define levels of preparedness for suppression operations, dispatching, issue of public warnings, and to restrict agricultural activities that might result in wildfire outbreaks. Implementing a new curing coefficient function into the GFDI equation that incorporates the findings from the present study will result in an increase in index values under partially cured conditions that might affect the current interpretation of the grass fire danger rating classes, particularly early in the fire season when grasslands are partially cured. The likelihood is that there will be an increase in the number of elevated fire danger days as a result of this change. As a result, any changes into the GFDI formulation need to be preceded by a comprehensive analysis of the effect and implications of the suggested changes in the fire potential, assessed primarily by comparison with historical norms.

It is also believed that further research is still required to understand the effect of the heterogeneity of curing at the landscape level on fire growth and suppression difficulty, and its implications on broad-scale fire danger rating.

Evaluation of the effect of fuel load on GFDI / Purton (1982) GFDI

Grass fuel load is now commonly used to estimate grassfire danger following Purton's (1982) adaptation of the McArthur (1977) Mk 5 fuel load function into the McArthur (1973) Mk 4 GFDI meter and which assumes a standard 4.5 t/ha fuel load for all grasslands.

The use of the Purton (1982) formulation is questionable following the evidence put forward in this report and in Cheney et al. (1993). We have not found an effect of fuel load in any fire behaviour quantity besides fireline intensity, which is a direct function of fuel load.

A number of fire experts have defended the use of Purton (1982) GFDI equation based on the perceived, but not quantified, direct effect of grass fuel load in (1) increasing in rate of spread; (2) increase fireline intensity; and (3) increasing flame height and suppression difficulty. In particular, there is a perceived capacity of the method to better capture the difficulty of control when fire danger rating is lower than Very High. Nonetheless, it is important to highlight that the calculation of the grassfire danger index through this variation violates the original GFDI formulation, resulting in an artificial increase or reduction of index values without regard to real fire potential. Figure 44 presents this artificial effect of fuel load on Purton's (1982) GFDI as compared with the original Mk 4 GFDI formulation (as per Noble et al. 1980). In a situation where the growing season leads to moderate grass growth, for example between 2 and 3 t/ha (well within the lower range of our experimental fires), Purton's modification will predict GFDI's around 50 when the general weather is suggesting an original GFDI around 100. This modification will lead to an under-estimate of the fire potential as it is well accepted that under such GFDI the effect of fuel structure is moderated. Conversely, Purton's modification can also lead to large over estimates of fire potential when the calculation is based on fuel loads that are 50% or 100% higher than the standardized 4.5 t/ha as originally suggested by McArthur.

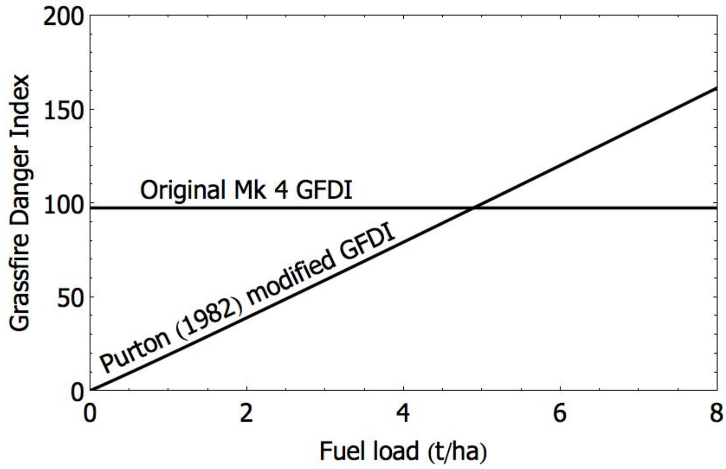

Figure 36. The effect of fuel load on GFDI as per Purton's (1982) formulation as compared with the original GFDI as per McArthur (1966) and Noble et al. (1980).

Table 10 further illustrates these issues by extending the analysis to a number of important fire behaviour characteristics associated with fire danger index. In Table 10 we analyse the relationship between the original GFDI and rate of fire spread, fire area after 30 min, fireline intensity and flame height, and how the Purton's GFDI is affected if fuel load is changed. The results show that only fireline intensity, which uses fuel load as a direct input, responds to changes in Purton's GFDI. The other fire behaviour quantities, namely rate of fire spread, fire growth and flame height, are independent of fuel load and thus Purton's GFDI.

This sensitivity analysis shows also that when comparing Purton's GFDI across different Mk4 GFDI values the results become contradictory. As two clear examples, for the first Mk 4 GFDI of 12, the Purton GFDI of 20 (fuel load of 8 t/ha) is paired with a fireline intensity of 18905 kW/m. When considering the base GFDI of 50, the Purton GFDI of 20 (fuel load of 2 t/ha) has an associated fireline intensity of about half of the example above (10658 kW/m). Further similar examples can be observed from the Table results, showing that Purton's GFDI is not a good descriptor of fire intensity.

Table 10. The effect of fuel load on Purton (1982) GFDI, grassfire behaviour and growth.

Fuel load (t/ha)	Rate of fire spread (m/min)	Fire area after 30 min (ha)	Fireline intensity (kW/m)	Flame height (m)	Purton GFDI
			Mk4 GFDI = 12		
		[air temp.: 22°C; relative humidity: 25%; 10-m open wind speed: 20 km/h]			
2	76	9.6	4726	2.9	5
4	76	9.6	9452	2.9	10

8	76	9.6	18905	2.9	20
Mk4 GFDI = 35					
[air temp.: 30°C; relative humidity: 17%; 10-m open wind speed: 30 km/h]					
2	144	88	8961	3.4	14
4	144	89	17992	3.4	28
8	144	89	35845	3.4	57
Mk4 GFDI = 50					
[air temp.: 30°C; relative humidity: 14%; 10-m open wind speed: 35 km/h]					
2	171	176	10658	3.6	20
4	171	176	21315	3.6	41
8	171	176	42630	3.6	83
Mk4 GFDI = 100					
[air temp: 30°C; relative humidity: 17%; 10-m open wind speed: 40 km/h]					
2	223	400	13845	3.9	40
4	223	400	27690	3.9	81
8	223	400	55379	3.9	166

Rate of spread calculation uses Cheney et al. (1998) assuming fully cured undisturbed grasses and dead fuel moisture content estimated as per Noble et al. (1980).

Fire area after 30 min assumes continuous fuels, no suppression action, an elliptical fire growth shape and a fire acceleration function of the form R_{ac} = R_{ss} x (1 - Exp[-0.05 x Time]); with R_{ac} being the accelerating rate of spread, R_{ss} the rate of spread at the pseudo steady state and Time is the time since ignition.

Another major issue with the use of the Purton GFDI is related to its use to inform public safety measures. The large discrepancies between the Mk 4 and Purton (1982) GFDI can lead to severe understatements of fire potential. In Table 10, for a GFDI of 100, a Purton GFDI of 40 is calculated for a grassland fuel load of 2 t/ha. This obviously can negatively impact the safety of rural communities. Conversely, the Purton's GFDI can lead to overstatements of fire potential when the grass fuel loads are assumed to be high. This again can lead to negative outcomes due to a high number of false alarms, which are known to lead to public distrust to warnings and complacency.

5 Conclusions

Understanding the effect of grassland fuel structure on fire behaviour is essential for the accurate estimation of fire potential and prediction of fire behaviour.

We carried out a large scale field-based experimental burning project over range of grassland fuel types to determine the effect of live fuel components, including their proportion and moisture content, on fire spread rate and behaviour in partially cured grasslands. We also used data from this study to investigate the effect of grass fuel load on fire behaviour. Finally we used our data to evaluate current grassland fire danger index metrics against observed fire behaviour.

A new fire spread curing coefficient function proposed earlier in this project was evaluated, and shown to provide adequate prediction capability and absence of bias. The function is considered a substantial improvement over previous ones used for southern Australia temperate pastures and grasslands. We recommend that this new function be implemented for operational prediction of grassland fire behaviour. It is important to note, however, that its applicability to grass regrowth situations and certain tropical grasslands remains to be determined.

Our analysis of the effect of fuel load on grassfire behaviour showed this variable to not influence fire rate of spread or flame height. Our results show also that extreme fire behaviour (characterised by fast rates of spread) will occur in low fuel load (e.g., between 0.15 and 0.25 kg/m2) grasslands, and fire-fighters should be aware of this important fire safety issue.

The present study also showed that the curing effect function used for fire danger rating in Australia can lead to an under-estimation of fire potential when fires occur under dry and windy conditions in partially cured grasslands. The results show the current fire danger formulation to under predict fire potential by a factor of three. The evaluation of the Purton (1982) GFDI fuel load function found this formulation to not be supported by data and to artificially bias the results, potentially leading to misleading fire danger warnings. A re-evaluation of the current system for fire danger is advised.

6 References

Adkins CW, Clements HB (1976) Photographic measurements of flame size over flat terrain. Functional Photography 11(6):32-34.

Albini, F.A. 1981. A model for wind-blown flame from a line fire. Combustion and Flame 43: 155-174.

Albini FA (1985) A model for fire spread in wildland fuels by radiation. Combustion Science and Technology 42, 229-258.

Alexander, M.E.; De Groot, W.J. 1988. Fire behavior in jack pine stands as related to the Canadian Forest Fire Weather Index System. Canadian Forest Service, Northern Forestry Centre, Edmonton, AB. Poster with text.

Alexander ME (1982) Calculating and interpreting forest fire intensities. Canadian Journal of Botany 60, 349-357.

Alexander, M.E. 2008. Proposed revision of fire danger class criteria for forest and rural areas in New Zealand. 2nd Edition. National Rural Fire Authority, Wellington, in association with the Scion Rural Fire Research Group, Christchurch. 62 p

Anderson SAJ, Anderson WR, Hollis JJ, Botha EJ (2011) A simple method for field-based grassland curing assessment. International Journal of Wildland Fire 20, 804-814.

Anderson, W.R., Cruz, M.G., Fernandes, P.M., McCaw, W.L., Vega, J.A., Bradstock, R.A., Fogarty, L., Gould, J., McCarthy, G., Marsden-Smedley, J.B., Matthews, S., Mattingley, G., Pearce, G. and van Wilgen, B.W. 2015. A generic, empirical-based model for predicting rate of fire spread in shrublands. Submitted to the International Journal of Wildland Fire 24, 443–460.

Andrews PL, Anderson SAJ, Anderson WR (2006) Evaluation of a dynamic load transfer function using grassland curing data. In: Andrews PL, Butler BW, comps. Fuels Management – How to Measure Success Conference Proceedings USDA Forest Service, Rocky Mountain Research Station. Proceedings RMRS-P-41. (Fort Collins, CO)

Babrauskas V (1984) Development of the cone calorimeter – a bench-scale heat release rate apparatus based on oxygen consumption. Fire and Materials 8, 81–95. doi:10.1002/FAM.810080206

Babrauskas V (2003) 'Ignition Handbook: Principles and Applications to Fire Safety, Fire Investigation, Risk Management and Forensic Science.' (Fire Science Publishers: Issaquah, WA).

Bradski G (2000) OpenCV. *Doctor Dobb's Journal* 25(11), 120-126.

Britton, C.M.; Karr, B.L.; Sneva, F.A. 1977. A technique for measuring rate of spread. J. Range Management 30(5):395-397.

Burrows ND, Ward B, Robinson A (1991) Fire behaviour in spinifex fuels on the Gibson Desert Nature Reserve, Western Australia. Journal of Arid Environments 20, 189-204.

Burrows ND, Ward B, Robinson A (2009) Fuel dynamics and fire spread in spinifex grasslands of the western desert. Pages 69-76 in (Tran C. Ed.) the Proceedings of the Royal Society of Queensland – Bushfire 2006 conference. Brisbane 6-9 June 2006.

Byram GM (1959) Combustion of forest fuels. In K.P. Davis (ed.). Forest Fire: Control and Use. McGraw-Hill Book Company, New York. pp. 61-89, 554-555.

Catchpole EA, Catchpole WR (1991) Modelling moisture damping for fire spread in a mixture of live and dead fuels. International Journal of Wildland Fire 1, 101-106.

CFA (2014) Grassland Curing Guide. Fire and Emergency Management, Country Fire Authority. (Burwood East VIC).Cheney NP, Just TE (1974) The behaviour and application of fire in sugar cane in Queensland. Australian Department of Agriculture, Forestry and Timber Bureau, Leaflet 115. (Canberra, ACT)

Cheney NP (1997) Effective grass curing on firespread and fire danger rating. In “Grass curing workshop”. 27 August, Aspendale, Victoria, Australia.

Cheney, N.P. 1990. Quantifying bushfires. Mathl. Comput. Modelling 13(12):9-15.

Cheney, N.P., Gould, J.S., Catchpole, W.R. 1993. The influence of fuel, weather and fire shape variables on fire-spread in grasslands. Int. J. Wildland Fire 3(1):31-44.

Cheney NP, Gould JS, Catchpole WR (1998) Prediction of fire spread in grassland. International Journal of Wildland Fire 8, 1-13.

Cheney NP, Sullivan AL (2008) Grassfires: fuel, weather and fire Behaviour, 2nd Edition. CSIRO (Collingwood, Victoria).

Cheney, N.P., Gould, J.S. 1995. Fire growth in grassland fuels. Int. J. Wildland Fire 5(4):237-247.

Clements, H.B.; Ward, D.E.; Adkins, C.W. 1983. Measuring fire behavior with Photography. Photogrametric Engineering and Remote Sensing 49(2):213-217.

Cruz, M.G., W.L. McCaw, W.R. Anderson, J.S. Gould, 2013. Fire behaviour modelling in semi-arid mallee-heath shrublands of southern Australia, Environmental Modelling and Software, 40:21-34.

Cruz M G., Gould J S., Kidnie S, Bessell R, Nichols D, Slijepcevic A (2015) Effects of curing on grassfires: II. Effect of grass senescence on the rate of fire spread. International Journal of Wildland Fire 24, 838–848.

Fire and Emergency Management (2014) Victoria Country Fire Authority (East Burwood, VIC).

Fosberg MA, Schroeder MJ (1971) Fine herbaceous fuels in fire danger rating. USDA Forest Service, Rocky Mountain Forest and Range Experimental Station Research Note RM-185. (Fort Collins, CO)

Kidnie S, Cruz MG., Gould J, Nichols D, Anderson W, Bessell R (2015) Effects of curing on grassfires: I. Fuel dynamics in a senescing grassland. International Journal of Wildland Fire 24, 828–837.

Luke RH, McArthur AG (1978) Bushfires in Australia. Australian Government Publishing Service. (Canberra, ACT)

Matthews S (2010) Effect of drying temperature on fuel moisture measurements. International Journal of Wildland Fire 19, 800-802.

Merrill, D.F., Alexander, M.E. 1987. Glossary of fire management terms. Canadian Committee on Forest Fire Management, NRCC №26516, Ottawa, Canada. 91 p.

McArthur AG (1966) Weather and grassland fire behaviour. Commonwealth of Australia, Forestry and Timber Bureau, Leaflet 100.(Canberra, ACT)

McArthur AG (1973) Grassland Fire Danger Meter Mk IV. Commonwealth of Australia, Forestry and Timber Bureau, Circular Slide-rule (Canberra, ACT)

McArthur AG (1977) Grassland Fire Danger Meter Mk V. Country Fire Authority of Victoria, Linear Slide-rule. (Melbourne, Victoria)

Noble IR, Bary GAV, Gill AM (1980) McArthur's fire-danger meters expressed as equations. Australian Journal of Ecology 5, 201–203.

Northcote KH, Beckmann GG, Bettenay E, Churchward HM, Van Dijk DC, Dimmock GM, Hubble GD, Isbell RF, McArthur WM, Murtha GG, Nicolls KD, Paton TR, Thompson CH, Webb AA, Wright MJ (1968). Atlas of Australian Soils, Sheets 1 to 10. With explanatory data (CSIRO Aust. and Melbourne University Press: Melbourne).

Parkes D, Newell G, Cheal D (2003) Assessing the quality of native vegetation: the 'habitat hectares' approach. Ecological Management & Restoration 4, S29-S38.

Purton CM (1982) Equations for the McArthur Mk 4 grassland fire danger meter. Meteorological Note 147, Bureau of Meteorology, 12 pp.

R Core Team (2014) 'R: A language and environment for statistical computing'.' (R Foundation for Statistical Computing: Vienna, Austria).

Rothermel RC (1972) A mathematical model for predicting fire spread in wildland fuels. US Department of Agriculture, Forest Service, Intermountain Forest and Range Experiment Station Research Paper INT-115, Ogden, UT. 40 pp.

Rothermel, R.C. 1991. Predicting behavior and size of crown fires in the Northern Rocky Mountains. Gen. Tech. Rep. INT-438, USDA For. Serv. Intermountain. For. and Range Exp. Stn., Ogden, Utah 46 p.

Sullivan AL, Gould JS, Cruz MG, Rucinski C and Prakash M. (2013) Amicus: a national fire behaviour knowledge base for enhanced information management and better decision making. MODSIM2013, 20th International Congress on Modelling and Simulation., Piantadosi, J., Anderssen, R.S. & Boland, J. (Eds.) , pp. 2068-2074.

Willmott, C.J. 1982. Some comments on the evaluation of model performance. Bulletin American Meteorological Society 63, 1309-1313.

Wotton BM, Alexander ME, Taylor SW (2009) Updates and revisions to the 1992 Canadian Forest Fire Behaviour Prediction Systems. Natural Resources Canada, Canadian Forest Service, Great Lakes Forestry Centre, Information Report GLC-X-10. (Sault Ste Marie, ON).

7 Appendix 1 - Point source fire growth experiments

A total of 26 point source fire growth experiments were conducted during this project with the bulk (20) being conducted at Braidwood, NSW. Due to the complexity of reducing and analysing these data only preliminary results for six Braidwood fires is presented here. These fire represent a cross-section of treatment and control with little variation in burning conditions. Table 11 summarises the conditions and overall spread rates of this subset of fires.

Table 11. Summary of burning conditions and overall spread rates from subset of point source fire growth experiments analysed.

Time of day (hh:mm)	Air temperature (°C)	Relative Humidity (%)	10-m open wind speed (km/h)	Curing level (%)	Overall fuel moisture content (%)	Duration (s)	Maximum cumulative rate of fire spread (m/min	Maximum interval rate of fire spread (m/min)
11:02 – 16:24	28-29	28-30	14.8-21.1	80-100	5.9-12.4	80-110	15.4 - 36.6	29.9 - 50.3

Figure 37 shows fire isochrones maps of two fires (E06 and S13) derived from the multi-step data reduction outlined in the Methods chapter, with each colour representing the distance covered in each spread interval. In these cases, the spread interval is 10 s. While shorter spread intervals could be used, overlap of fire isochrones resulting from slight errors in image rectification or incorrect locating of fire edge diminishes the utility of such fine temporal resolution. Furthermore, shorter spread intervals may not provide an adequate averaging period for experimental variables such as wind speed. Digitisation of isochrones stopped when the fire perimeter was determined to have been affected by suppression or by impacting the plot boundary.

From these maps, additional fire behaviour metrics were determined for each spread interval, including distance travelled, fire area, fire perimeter length, rate of change of these (at both the per interval and per unit level), headfire width, fire length, fire breadth, as well as rate of fire spread.

Distance travelled (and thus rate of spread) was considered in two ways: cumulative distance (the total distance the fire had travelled from ignition at each interval) and interval distance (the distance the fire had travelled since the last interval. While these can produce similar results, in many cases they are significantly different. Figure 38 illustrates the difference between cumulative distance and interval distance in E06 in the eighth interval. For the purposes of this report, only interval distance will be presented.

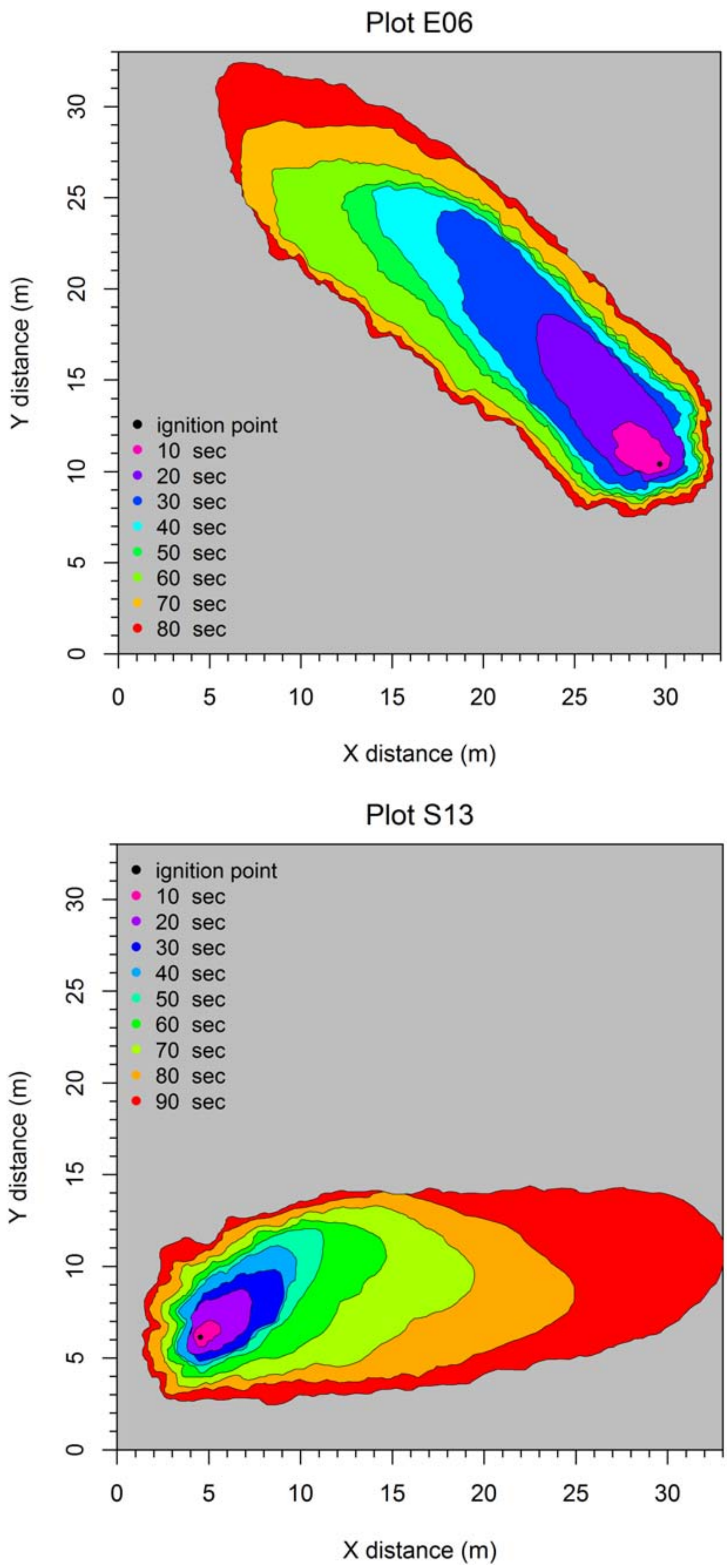

Figure 37. Examples of two isochrones maps, one for E06 (top) and one for S13 (bottom). The isochrones interval was fixed at 10 s. The total number of isochrones depends on the speed of the fire and when it reached a plot boundary.

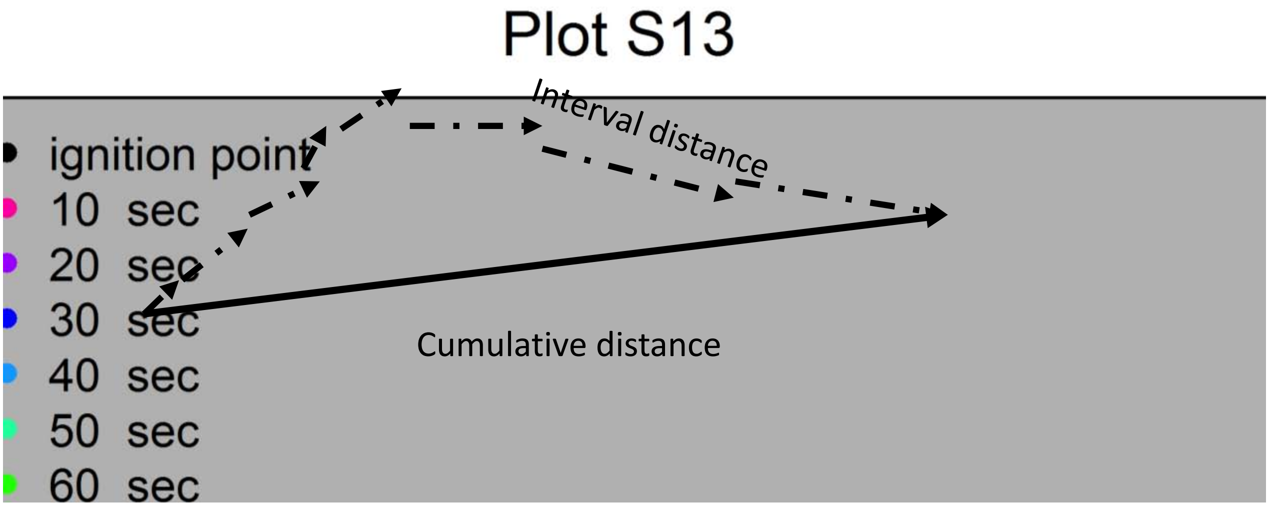

Figure 38. Illustration of difference between cumulative distance and interval distance in E06. Cumulative distance is essentially the vectorial sum of the interval distances but in this case, because of the major shift in wind direction in the sixth interval, cumulative distance is much shorter than the scalar sum of the interval distances and thus will result in a lower overall rate of spread at this interval.

Headfire width (Cheney *et al.* 1993) is defined as that distance across which the head of the fire extends and from which flames generally tend to lean consistently over unburnt fuel. Figure 39 illustrates this concept on the isochrones map of S03 for intervals 7 and 9.

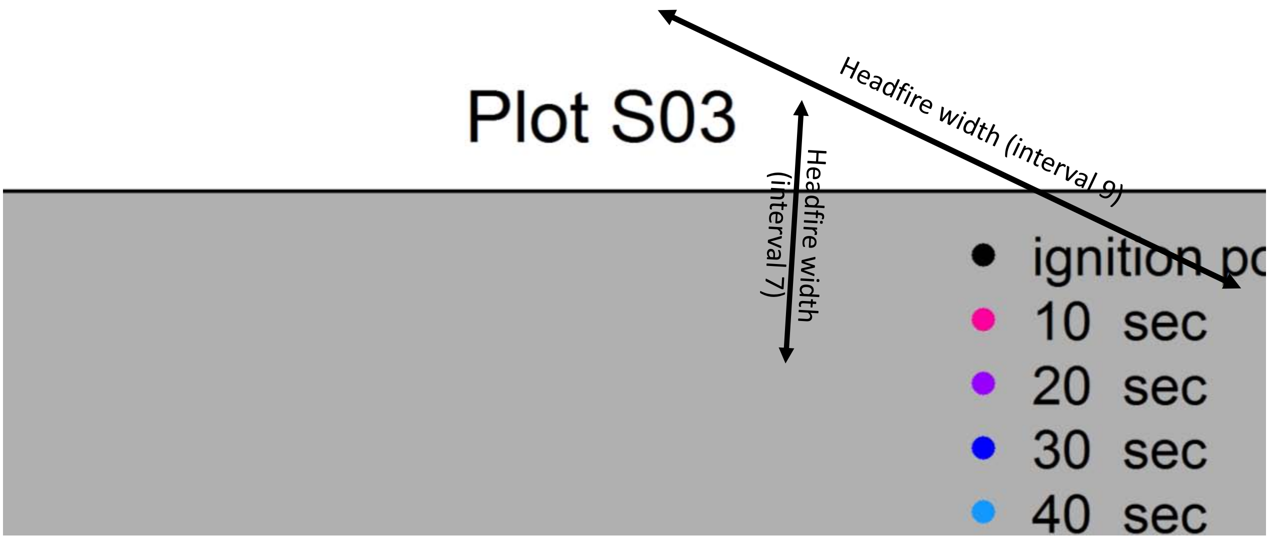

Figure 39. Illustration of headfire width for two intervals in fire S03.

Figure 40 summarises the changes in fire area, fire perimeter length, headfire width and length:breadth ratio over time for all six fires.

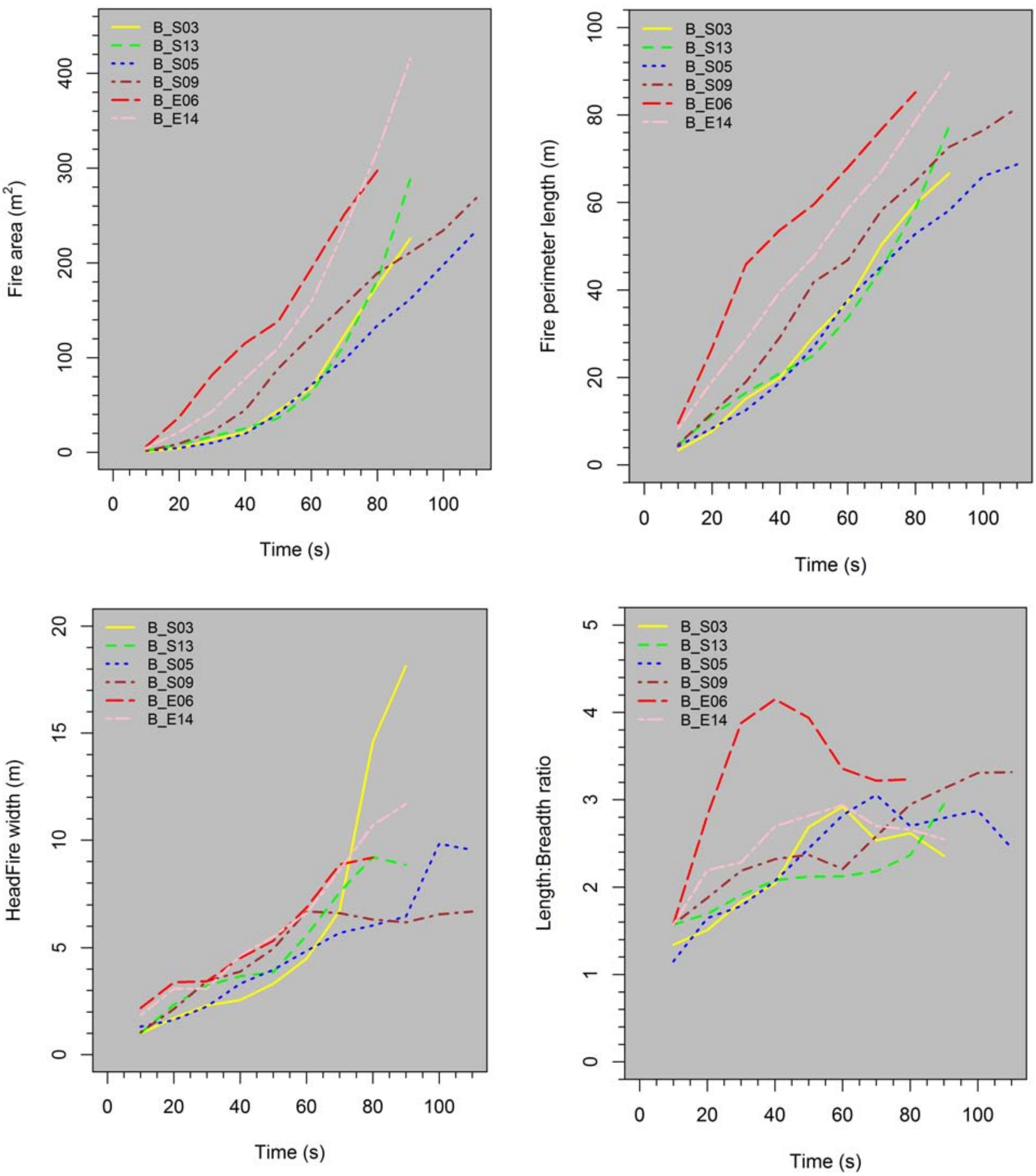

Figure 40. Various fire behaviour and fire shape metrics for the six point ignition fires thus far analysed. Clockwise from top left: fire area, fire perimeter length, length:breadth ratio and headfire width.

Fire E14 grew to cover the most area and longest perimeter before it reached a plot edge (total area of each experimental plot is 900 m^2). Its rate of increase of area followed an exponential like growth curve where as its perimeter length growth was very linear. This was driven predominantly by a gradual shift in wind direction of about 40 degrees over the 90 seconds of its spread. The growth in headfire width was similarly linear whereas its change in length to breadth ratio peaked around 60 seconds as the changing wind direction increased the fire's width after this.

Once established, all fires exhibited similar rates of increase of area, perimeter and headfire width (with the exception in the latter case of S03 which had a dramatic increase in headfire width as a result of a significant change in wind direction as illustrated in Figure 39. S13 also exhibited a rapid increase in fire area in the last two intervals but this does not appear to have been the result of a change in wind direction but rather speed. All fires exhibited highly variable length:breadth ratios throughout the experiments. Four fires (S03, S05, E06, E14) appear to asymptote to slightly lower ratios after peaking 40 to 60 seconds after ignitions.

Figure 41 (left) shows the time rate of change in the area for each fire. Fires S13 and E14 exhibited very similar rates of change in area toward the end of each experiment. At this point, each fire was increasing in area at a rate of 10 m^2 per second, primarily driven by the rate of spread of each fire rather than any dramatic changes in wind direction. This means that in 10 seconds, each fire would increase in size by about 100 m^2, however as this rate is increasing at the end of these experiments, it is likely that such fires would cover even larger areas in this time.

S09 and S05 had the lowest rate of area increase at ~3.5 m^2/s which seems to have been quite consistent over the final 4-5 intervals. This is consistent with these fires being the slowest.

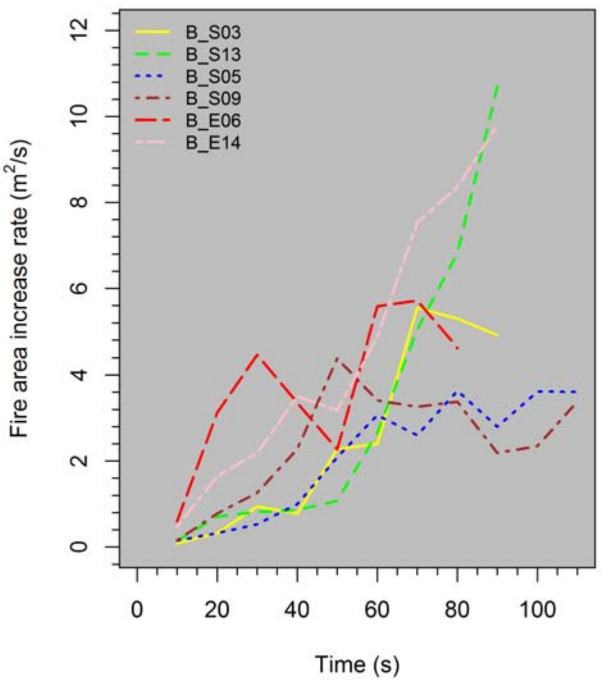

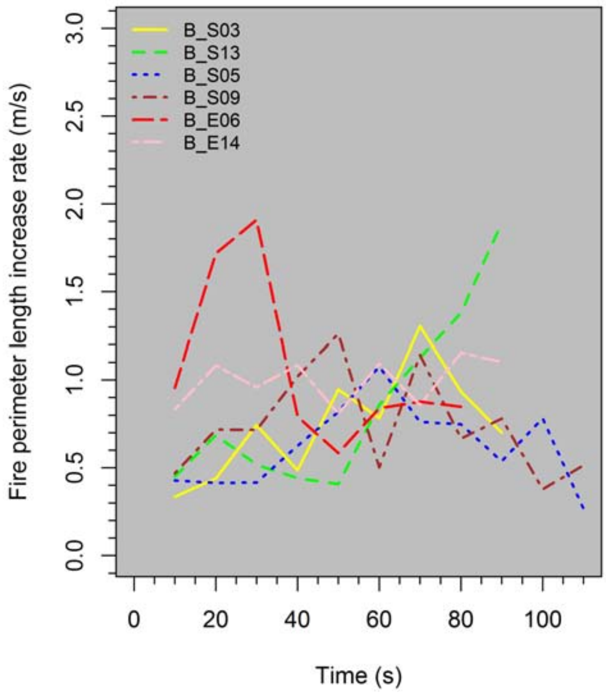

Figure 41. Time rate of change of the area and perimeter length for each fire.

Figure 41 (right) shows the time rate of change of the perimeter length for each fire. As with rate of area increase, fire S13 exhibits the fastest increase in perimeter length at the end of the fire experiment at ~1.8 m/s, however, E14's rate of perimeter length increase is fairly static at around 1.0 m/s. S05 and S09 exhibited decreasing rate of perimeter length increase.

It is expected that the rate of area increase of a fire will asymptote to a constant value once the fire reaches its quasi-steady rate of spread unless there is a major change in spread direction as a result of a significant wind shift. Perimeter increase should continue to increase exponentially but this too should begin to drop off as the length of actively spreading fire edge becomes a smaller percentage of the total perimeter length. For fire suppression planning, a metric that captures the rate of increase of the most active zones of fire may be more useful than a metric covering the entire fire perimeter.

Figure 42 shows a plot of the interval rates of forward spread for all six point ignition fires. All interval rates of forward spread exhibit a high degree of variability, most likely driven by variability in wind strength and direction as a result of turbulent eddies in the boundary layer flow.

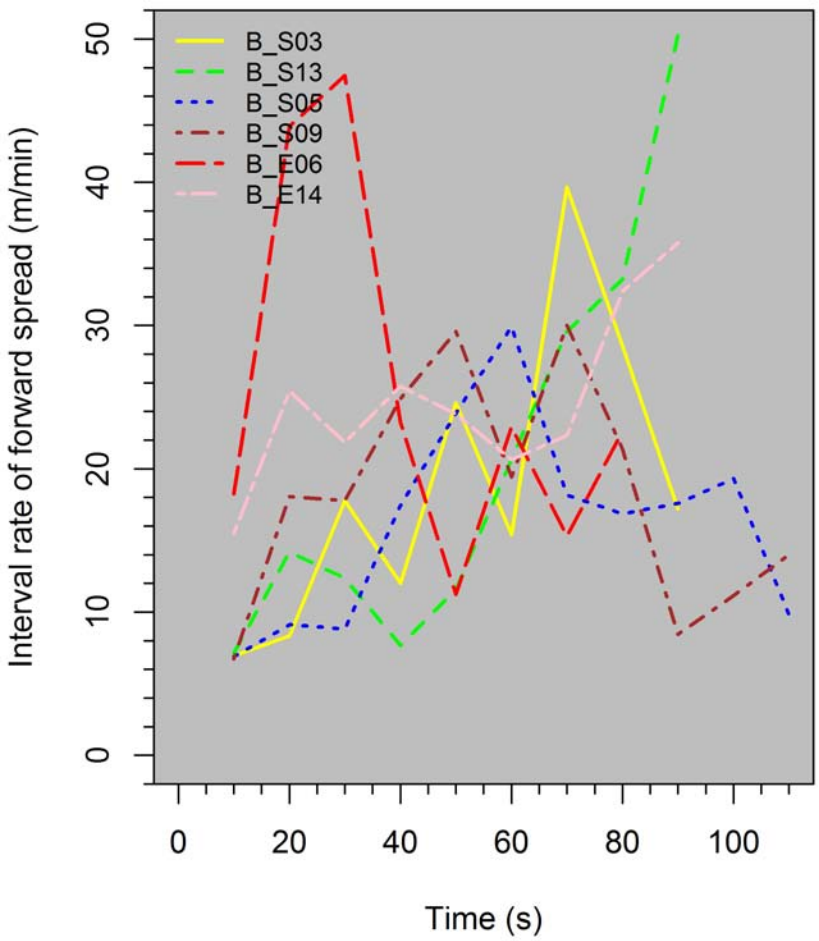

Figure 42. Plot of interval rates of forward spread for all six point ignition fire growth experiments. These rates of spread are highly variable. While they appear to be relatively very high, they are of short duration.

S13 exhibited the fasted interval rate of spread of 50.3 m/min which occurred right at the end of the experiment and followed five periods of steadily increasing rate of spread (which started at interval 4 with a rate of forward spread of 7.7 m/min. This is commensurate with this fire's increase in area and perimeter length. Fire E06 reached a similar speed (47.5 m/min) at interval 3 but then decreased over the following five periods to an average of 18.0 m/min. Most fires exhibited acceleration from ignition but do not appear to have reached any quasi-steady state condition in regard to rate of forward spread. S09 and reached peak interval speeds of around 30 m/min but slowed significantly toward the end. S03 exhibited highly variable speeds with rapid changes in speed but an overall steady increasing trend.

The highly erratic nature of the fire interval rate of forward spread is best captured by considering the time rate of change of interval fire speed, which is essentially the acceleration exhibited during each interval. Figure 43 shows the time rate of change of the interval forward rate of spread for each fire. This metric shows whether the speed of the fire is increasing or decreasing. An acceleration of zero means that a fire's speed is constant. The units presented here are m/min/sec and details the average change in the speed of the fire given in m/min per second during an interval.

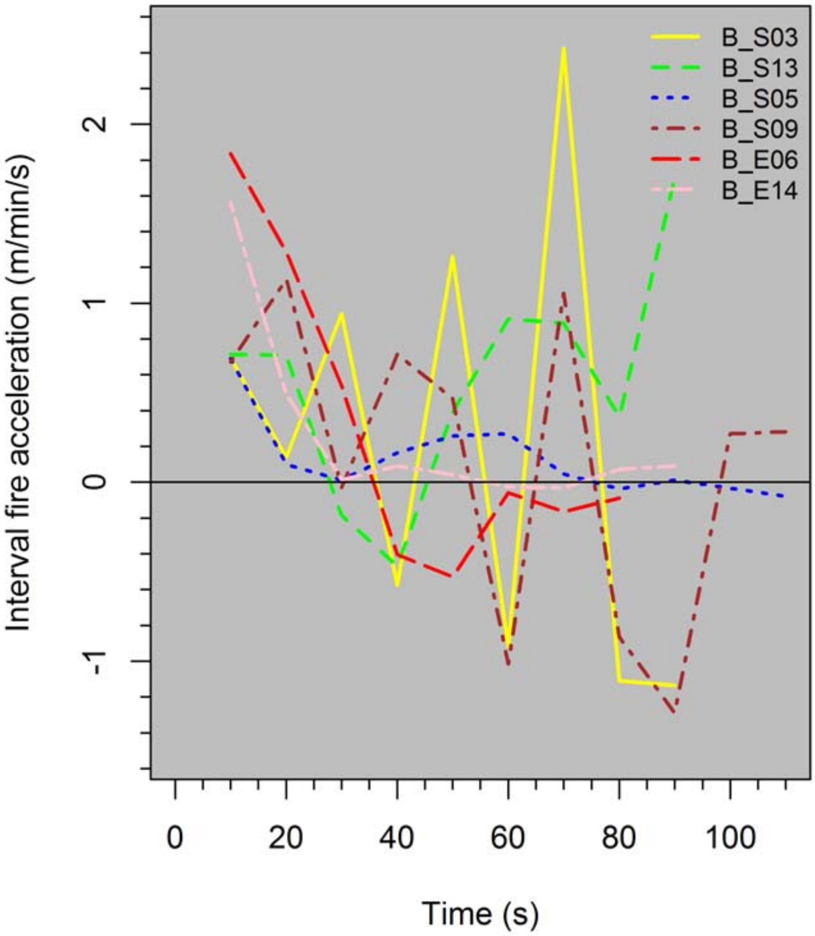

Figure 43. Time rate of change of interval rate of forward spread (i.e. acceleration) for each fire. Zero acceleration means that a fire's speed is constant.

The fire that exhibited the highest acceleration and deceleration is clearly S03 as suggested by Figure 42. This fire's peak acceleration was ~2.4 m/min/s. Its fastest deceleration was ~-1.0 m/s. Essentially this fire oscillated each interval between acceleration and deceleration. However, as shown in Figure 42, the magnitude of the accelerations outweighed the magnitude of the decelerations to ensure that the fire's speed basically kept increasing over the life of the fire. Similar degrees of variability were exhibited by S09 and S13. S05 showed a general trend toward deceleration to a static (i.e. zero acceleration) rate of forward spread. E06 started with high acceleration (1.8 m/min/s) in interval 1 but its acceleration then consistently decreased over the next three intervals until it began to decelerate.

The primary objective of the point source fire growth experiments is to develop a model that describes the rate of increase (acceleration) of the rate the spread of a new ignition until it reaches its quasi-steady rate of spread. Figure 44 shows the interval rate of forward for each fire normalised against the quasi-steady rate of spread predicted for the prevailing conditions by the CSIRO Grassland Fire Spread Meter (Cheney et al. 1998) as given in Amicus (Sullivan et al. 2013).

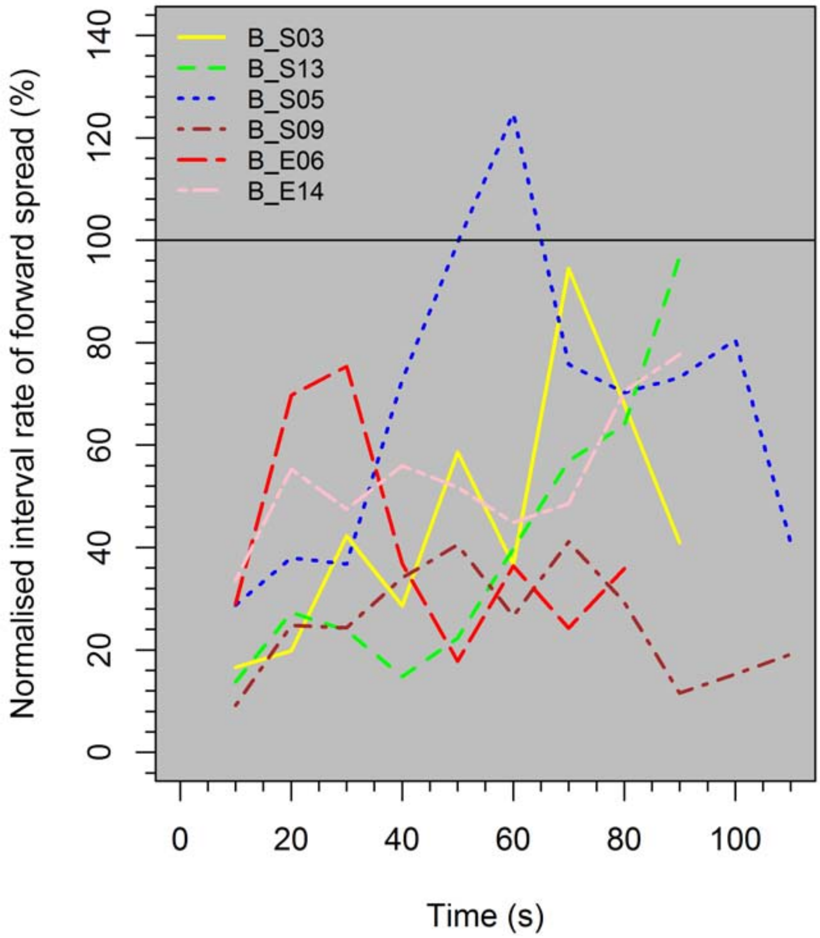

Figure 44. Interval rate of forward spread of each fire normalised against the predicted quasi-steady rate of spread given by Cheney et al. (1998). 100% means the fire has achieved the quasi-steady rate of spread.

With the exception of one interval for fire S05, none of the fires achieve the quasi-steady rate of spread predicted by Cheney et al. (1998). However, most fires (e.g. E14, S13, S03) are accelerating toward this value but over the distance available have not yet reached it. S03 and S13 exhibit the greatest potential to do this if conditions did not vary. Fire S05 briefly exceeded the quasi-steady rate of spread before slowing. This is most probably due to the fact that this fire was in partially cured (80%) pasture and as has been detailed elsewhere in this report, the curing coefficient function of Cheney et al. (1998) under predicts the rate of spread of fires in such fuels.

Neither S09 nor E06 provide any indication in the space available for the experiments that they would attain the quasi-steady rate of spread; S09 primarily because its headfire width remained narrow at the end (<7 m), E06 because its length:breadth ratio was decreasing (Figure 40).

Discussion

Preliminary analysis of the data collected during the fire growth and build up phase of point ignitions is still underway. Results presented here showed that the fires conducted in the 33 m × 33 m plots were spreading at below the quasi-steady rate of spread predicted by the CSIRO Grassland Fire Spread Model (Cheney et al. 1998). However, a number of fires exhibited rapid acceleration in the first few intervals that suggests that these fires would have attained such as fire spread rate if allowed to spread for an additional few minutes. More conclusive results should be forthcoming when all data reduction for these experimental fires has been completed and analysis conducted.

The development of a model to predict the build-up time to quasi-steady state is critical to understanding the time available to suppression crews for successful initial attack and for high fidelity landscape fire spread prediction. In the latter instance, build up time is not just applicable to new fire outbreaks but also for break-aways from existing fire perimeters and fire spread through ‘choke’ points where fire width is constrained due to suppression action or changes in fuel condition. Once all point ignition fire growth experiments have been processed to provide information about fire interval rate of spread, acceleration and time rate of change of area and perimeter, all fire behaviour and environmental conditions will be analysed to determine the feasibility of developing a generally applicable fire growth model.

Key environmental variables in this data analysis and model development are likely to be wind gust magnitude, frequency and duration, standard deviation of wind direction (i.e. sigma theta), grass curing and fuel moisture content. Understanding the spatial and temporal relationships between the fire and anemometer will be essential to providing prognostic capability in such a model.

CONTACT US

t 1300 363 400
+61 3 9545 2176
e enquiries@csiro.au
w www.csiro.au

YOUR CSIRO

Australia is founding its future on science and innovation. Its national science agency, CSIRO, is a powerhouse of ideas, technologies and skills for building prosperity, growth, health and sustainability. It serves governments, industries, business and communities across the nation.

FOR FURTHER INFORMATION

CSIRO Land and Water
Miguel Cruz
t +61 2 6246 4219
e Miguel.cruz@csiro.au
w www.csiro.au